CFD BASED PERFORMANCE ANALYSIS OF REACTION TURBINE

A DISSERTATION

Submitted in partial fulfillment of the requirements for the award of the degree of

MASTEER OF TECHNOLOGY

in

ALTERNATE HYDRO ENERGY SYSTEMS

By

SILADITYA BAG

ALTERNATE HYDRO ENERGY CENTRE
INDIAN INSTITUTE OF TECHNOLOGY ROORKEE
ROORKEE-247667 (INDIA)

MAY, 2016

Candidate's Declaration

I hereby declare that the report which is being presented in this work **"CFD based performance analysis of reaction turbine"** in partial fulfilment of the requirements for the award of the degree of **Master of Technology** in Alternate Hydro Energy Systems, submitted in **Alternate Hydro Energy Centre, Indian Institute of Technology, Roorkee** is an authentic record of my own work carried out during a period from July 2015 to May 2016 under the supervision of **Dr. M.K.Singhal**, Senior Scientific Officer, AHEC Department, Indian Institute of Technology, Roorkee and **Dr. R.P.Saini**, Professor, Alternate Hydro Energy Centre, Indian Institute of Technology, Roorkee.

I have not submitted the matter embodied in this report for the award of any other degree or diploma.

Date: May, 2016 (Siladitya Bag)

CERTIFICATE

This is to certify that the above statement made by the candidate is correct to the best of my knowledge.

Dr. M.K.Singhal

Senior Scientific Officer,

AHEC Department,

Indian Institute of Technology,

Roorkee-247667

Dr. R.P.Saini

Professor,

AHEC Department,

Indian Institute of Technology,

Roorkee- 247667

ACKNOWLEDGMENT

I would like to express my sincere gratitude to my supervisors, **Dr. M.K.Singhal**, Senior Scientific Officer, Department of AHEC, Indian Institute of Technology, Roorkee and **Dr. R.P.Saini**, Professor, AHEC, Indian Institute of Technology, Roorkee for their valuable guidance, support, encouragement and immense help.

I also express my deep and sincere sense of gratitude to **Dr. M.P.Sharma**, Head, AHEC, Indian Institute of Technology, Roorkee for his motivation and full cooperation during the progress of work.

I am also grateful to all faculty members and staff of Alternate Hydro Energy Centre, Indian Institute of Technology, Roorkee.

I extend my thanks to all my friends who have helped directly or indirectly for the completion of this progress report.

Finally, I would like to express my deepest gratitude to the Almighty for showering blessings on me. I gratefully acknowledge my heartiest thanks to all my family members for their inspirational impetus and moral support during the course of work.

Date: (SILADITYA BAG)

ABSTRACT

India is one of the fastest growing economy in the world. And energy plays a vital role in the development of country's economy. Day by day the gradual crisis of electricity and pollution from conventional energy sources influence to diversify our source of energy. Hydro power is one of the cleanest form of energy sources in the world. India has a vast amount of small hydro potential, and most of the potentials are located in northern and north-eastern states.

As discharge and head determine the capacity of a hydropower plant and plant capacity formulates the design of a hydro-turbine, therefore turbine designing always needs apt attention to produce optimal design. To get better accuracy in designing, it is always needed to study flow analysis data of a turbine model under similar environment as proposed site.

As testing the prototype of hydro turbine in laboratory is tedious, time consuming and costly process, it is therefore convenient to perform the whole process under Computational Fluid Dynamics (CFD) environment, which not only reduces experimental cost, but also reduces time consumption.

Under present investigation, a CFD based performance analysis of reaction turbines has been carried out. An attempt has been made to compare the simulation results with experimented results in a Francis turbine full-scale model by using RNG κ-ε turbulence model. A comparison study has been done between working turbine setup and CFD model to demonstrate the efficiency variation under different load conditions. The torque produced by the turbine under different discharge conditions has been computed through ANSYS Fluent flow simulation solver. The graphical and tabular representations of efficiency have been included for better understanding of the turbine setup. It has been observed that RNG κ-ε turbulence model has great level of accuracy which predicts maximum achievable efficiency of 94.10% from that Francis turbine setup. The computation process also has represented the velocity contour and pressure contour in the flow circuit with a brilliant GUI representation. Which additionally helps to identify the critically flowing zone and cavitation prone area in the hydraulic circuit. In conclusion, the relevance of CFD based performance study and their limitations has been discussed. The future scope on this relevant field has also been concluded at the end of the study.

CONTENTS

LIST OF FIGURES

LIST OF TABLES

NOMENCLATURE

Symbols

h	Head(m)
Q	Discharge(m^3/s)
N	Speed(RPM)
V	Speed(m/s)
Ns	Specific Speed
p	Pressure(N/m^2)
V,U	Velocity(m/s)
D	Diameter of runner(m)
d	Diameter of penstock(m)
B	Width of runner(m)
t	Time(sec)
σ	Yield Strength(N/mm^2)
n	Number of blades
ρ	Density(kg/mm^3)
μ	Dynamic Viscosity($N\text{-}s/m^2$)
ν	Kinematic Viscosity(m^2/s)
T	Thickness of blade(m)
E	Energy(Watt)
g	Acceleration due to gravity
Cp	Pressure Coefficient
ω	Angular speed(/s)
R	Radius of Runner
δ	Some constant
θ	Angle in(Degree)
κ	Turbulent Kinetic Energy
ε	Turbulent Dissipation
ω	Specific Rate of Dissipation

Abbreviations

kW	Kilowatt
MW	Megawatt
RPM	Revolution Per Minute
GHG	Green House Gas
CEA	Central Electricity Authority
MNRE	Ministry of New and Renewable Energy
CAD	Computer Added Design
CFD	Computational Fluid Dynamics
RANS	Reynolds Averaged Navier Stokes
SAS	Scale Adaptive Simulation
LES	Large Eddy Simulation
RNG	Re-Normalization Group
SRS	Scale Resolving Simulations
DES	Detached Eddy Simulation
WMLES	Wall Modelled Large Eddy Simulation
SAS-SST	Scale Adaptive Simulation-Shear Stress Transport
PAT	Pump As Turbine
FDM	Finite Difference Method
FVM	Finite Volume Method
FEM	Finite Volume Method
URANS	Unsteady Reynolds Averaged Navier Stokes
RAM	Random Access Memory
GPU	Graphics Processing Unit
GUI	Graphical User Interface

CHAPTER 1

INTRODUCTION AND LITERATURE REVIEW

1.1 INTRODUCTION

From the inception of civilization, when human being first realize the elegance and welfare of science by discovering fire, the wheel of progress had set out its journey since then. Mankind achieved numerous discoveries to nurture their curiosity and conquered adversities for the betterment of standard of living. And discovery of electricity is a monumental achievement in the history of civilization. In this 21st century we not only judge a nation by its per capita income but also we compare one another by our per capita energy consumption as well. And it is a great challenge to our modern science to harness energy with more sustainable and intelligent way. India as a fast developing country is now breaking through a crucial period of time when it is experiencing immense crisis of electricity in all vital sectors like agricultural, manufacturing, construction, trade and domestic etc. Our annual generation of electricity vastly depends upon coal based power pants. According to ecological point of view and due to some major threats from conventional energy sources, we need to diversify our source of energy generation.

Hydropower is the kind of renewable energy source which contributed over 16% of global electricity demand as on 2008[1]. It is the only form of renewable energy which can compete with conventional energy sources according to its generation potential. Our continent Asia is consecrated with numerous rivers which are majorly fed with molten glaciers and monsoon rain water. Currently Asia possess approximate installed capacity of hydropower by 29% [2] with respect to global install capacity.

According to Central Electricity Authority of India, our country has 148700MW exploitable potential of hydropower by ranking 5th globally [2]. Currently, India has 46880.24MW generation capacity of hydropower, contributing 16.24% of total electricity generation of the whole nation, as on Feb 29st 2016[3].

Although we have exploited only about 31% of total potential of hydropower, but the remaining needs special attention and challenging civil works. National Hydroelectric Power Corporation (NHPC), Northeast Electric Power Company (NEEPCO), Sutlej Jal Vidyut Nigam (SJVN), Tehri Hydro Development Corporation Ltd (THDC), NTPC-Hydro, Damodar Valley Corporation

(DVC) are the few major public sectors, engaged in development of large hydro in India. Although hydropower plants are ecologically clean and much safer than coal based power plants but due to some major environmental issues like GHG emission from reservoir, disturbance of human and fauna habitat, diversion of water ways, fish migration problem and above all a huge initial capital investment made it less popular.

To encourage investors from various sectors, government of India has set top priority to harness small, mini and micro hydropower to fillip the green energy revolution under the flagship of Ministry of New and Renewable Energy. Some of the notable Government nodal organizations like Indian Renewable Energy Development Agency (IREDA) and premier institute like Alternate Hydro Energy Centre (AHEC-IIT Roorkee) are dedicated to cultivate hydropower in an easier and affordable way. The hydropower projects in India are broadly classified in to large hydro and small hydro. Projects beyond 25MW of capacity are considered as large hydro and small hydro projects are recommended from 25MW to 2MW of potential according to MNRE norms. The CEA report on energy generation reveals that hydropower contributes about 16.24% [3] of electricity generation nationwide. And small hydro contributes about 8.91% [3] of total hydro power generation and only about 1.44% of total energy generation nationwide. The contribution of small hydro power in renewable energy sector is about 11%, succeeded by wind (64.62%), solar energy (12.57%) and BM power/cogeneration (11.72%) as on 29th Feb 2016[3].

A study has been made to show the relevance and significance of different renewable sectors in our country for better understanding as shown in the Table 1.1 and in Fig 1.1.

Table 1.1: All India installed capacity (MW) of power stations [3]

MODE WISE BREAKUP								
THERMAL			NUCLEAR	LARGE HYDRO	RES(MNRE)			
COAL	GAS	DIESEL			SMALL HYDRO	WIND POWER	BIO-MASS	SOLAR POWER
175857.8	24508.6	993.5	5780.00	41997.42	42703.42	25088.19	4677.63	4878.87

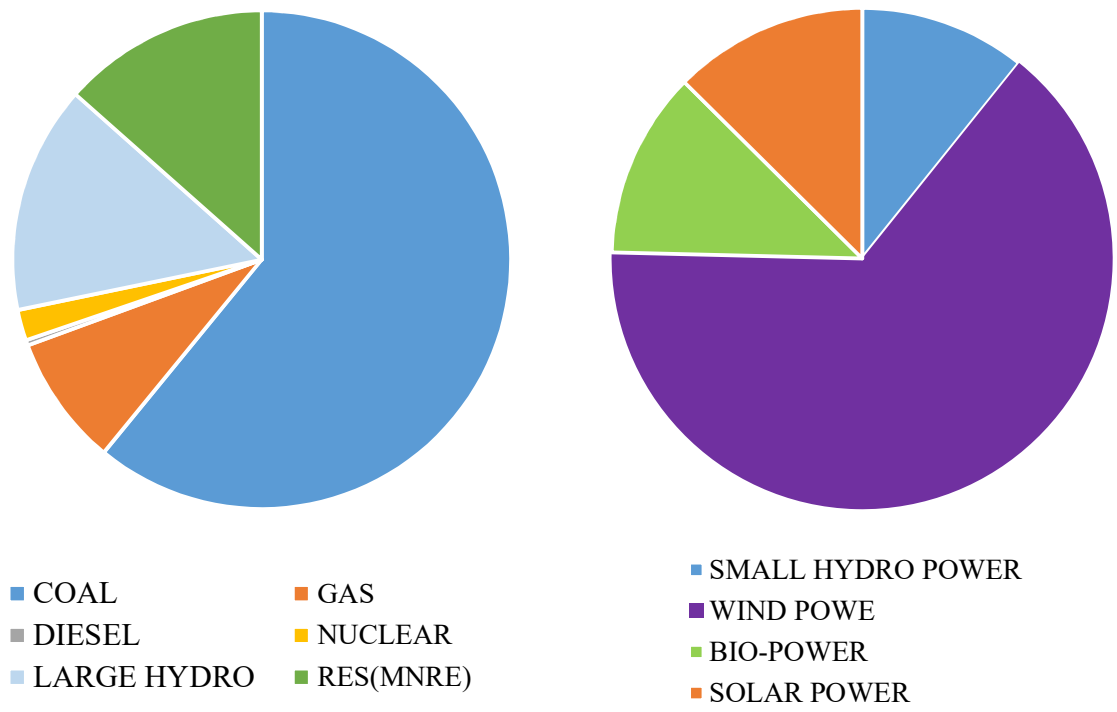

Fig 1.1 Pie chart of different power sources [3]

The above pie-charts are drawn from CEA report on generation capacity of different power sources for better understanding of present renewable and hydropower scenario in India. The comparison study of CO2 emission from different source of energy is graphically drawn in the Fig 1.2.

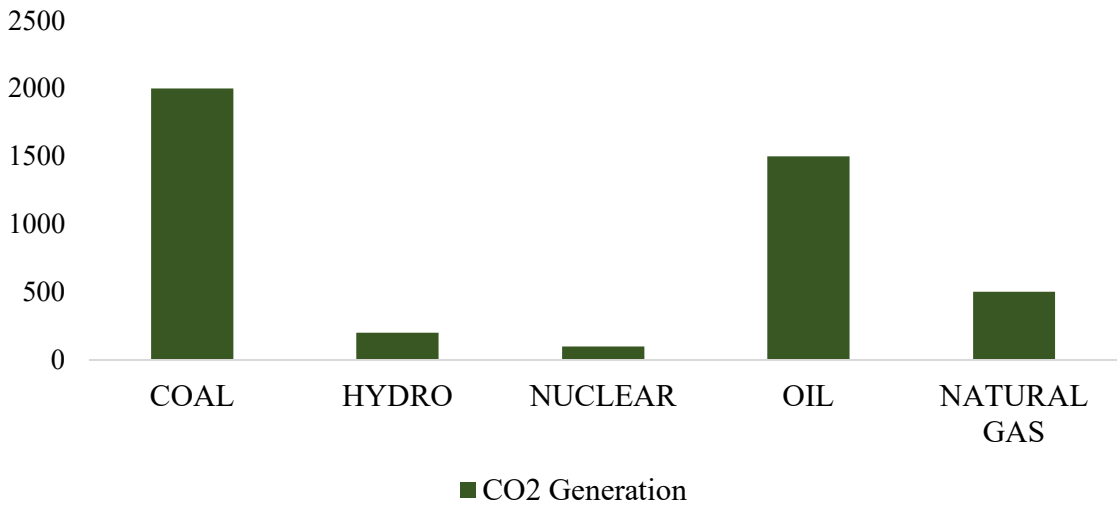

Fig 1.2 CO2 Equivalent emission from different energy sources [4]

As in India, water is an issue of state government therefore the major hydro projects are operated and owned by state governed agencies. A comparison study on development of hydro projects between the year 2008 and 2014 has been shown in the Fig 1.3.

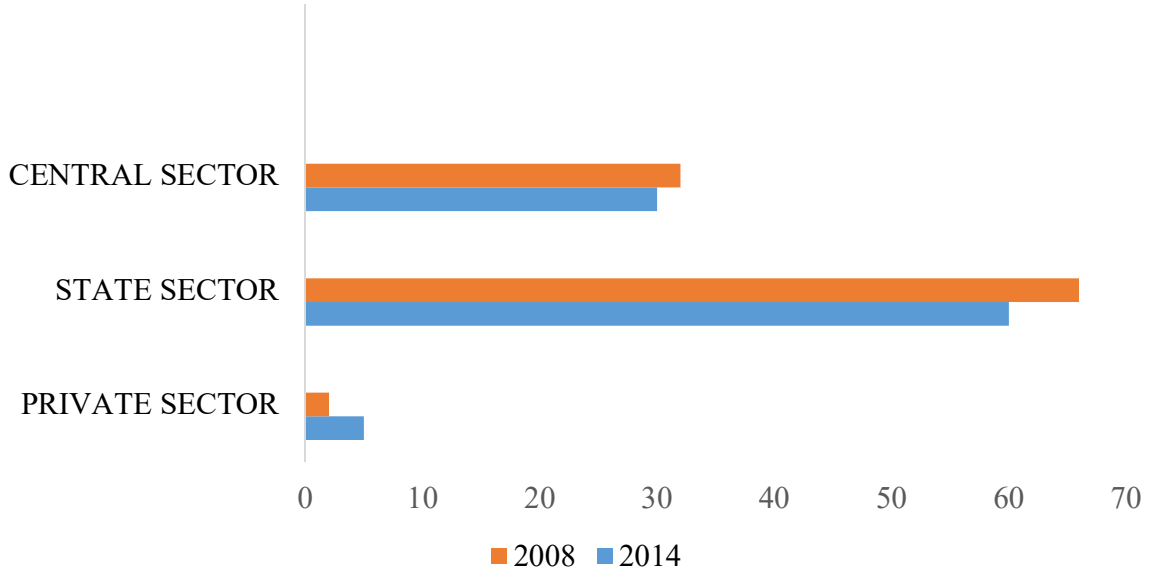

Fig 1.3 Share of central, state and private sector in hydropower in 2008 and 2014 [4]

1.2 SMALL HYDRO POWER

Although there is no international consensus for small hydro, but the major small hydro power harnessing countries follow a similar standard for small hydro. In Canada the small scale hydro refers from 20 to 25MW. Similarly, in US the potential up to 30MW is considered as small hydro and in India, ministry of new and renewable energy (MNRE) has set upper limit of Small hydro up to 25MW and lower limit of 2MW. In India the hydropower sector, under MNRE is divided in to three different sub category, as given in Table 1.2.

Table 1.2: Norms for different types of hydro scheme in India [5]

Type	Plant capacity in kW
Micro hydro	Up to 100
Mini hydro	101-2000
Small hydro	2001-25000

1.2.1 Advantages of Small Hydro in India

Apart from flexibility and reliability of Small hydro scheme, it has been proven the best form of renewable energy source for remote areas. In India, the major small hydro projects need not have environmental clearances due to its environment friendly operation. Moreover the administrative approval from New and Renewable Energy, for the year of 2014-15 and the remaining period of 12th pan for small hydro program has made the SHP schemes more attractive for different sects of developer. The schemes are shown in the Table 1.3.

Table 1.3: Central financial assistance scheme for SHP [5]

Scheme	Beneficiary
Resource assessment and support for identification of new sites.	State govt. dept. Agencies/local bodies in govt. sector.
Setting up new SHP Projects in the private / co-operative / Joint sector etc.	Private sector, Joint sector, Co-operative sector. Etc.
Setting up new SHP Projects in the Government/ state sector.	Government/State/Public sector ran by govt. dept./agencies/SEBs/local bodies.
Renovation and Modernisation of existing SHP projects in the Government sector.	Up to 25 MW of SHP, commissioned at least 7year prior to date of submission of proposal to the ministry.
Development/upgradation of Water Mills (mechanical/electrical output) and setting up Micro Hydel Projects up to 100 kW capacity	State govt. dept. /state nodal agencies/co-operatives/local bodies/tea gardens/industrial entrepreneur/NGOs. Etc.
Research & Development and Human Resource Development.	R&D depts. Taken by government bodies/Agencies/PSUs/Co-operatives/Autonomous agencies (like AHEC).

1.2.2 Significance of Small Hydro Project in India

India accounts a glorious history of small hydro power of more than 100 years. The first hydro project of 130kW observed by India was at Sidrapong (Darjeeling) in the year of 1897, which is running well till date with improved and re-commissioned potential of 600kW. Northern India has three major river basins (Indus, Ganga, and Brahmaputra) which are not only enriched with agricultural activities but also promise a vast amount of hydro potential.

From MNRE database, the state-wise potential of small hydropower is given in the Table 1.4.

Table 1.4: Small hydro potential in major states with more than 900MW [6]

POTENTIAL, INSTALLED & UNDER IMPLEMENTATION (as on31.03.2014)							
Sl. No.	**State**	**Potential**		**Projects Installed**		**Project under implementation**	
		Nos.	**Total Capacity (MW)**	**Nos.**	**Capacity (MW)**	**Nos.**	**Capacity (MW)**
1	Andhra Pradesh	387	978.40	68	221.03	13	32.04
2	Arunachal Pradesh	677	1341.38	149	103.905	44	22.23
3	Chhattisgarh	200	1107.15	9	52.00	4	115.25
4	Himachal Pradesh	531	2397.91	158	638.905	33	76.20
5	J&K	245	1430.67	37	147.53	7	17.65
6	Karnataka	834	4141.12	147	1031.658	23	173.09
7	Uttarakhand	448	1707.87	99	174.820	46	174.04

There are many other states which are enriched with small hydro potentials but are not enlisted here. Cumulatively there are about 6474 numbers of sites with 19749.44MW of potentials all over the India, of which 3803.678MW of potential has been implemented under operation and 895.40MW of potential is under construction till 31st March 2014 [6].

1.2.3 Disadvantages and Constraints of Small Hydro Power

The basic characteristics of a small hydro scheme is its remote location in a hilly area which is why the investors are discouraged due to its geographical inaccessibility. On the other hand the initial investment and construction period are very high. As the turbine design and selection is depended upon the head and discharge data of the particular site therefore every design and equipment are site specific which incurs project cost is very high. Moreover the gestation period for a hydro project is comparably longer than other energy projects. Therefore the hydro project development from privet sector is significantly low. Therefore to eliminate these shortcomings and optimize the proper utilization of resources there are various approaches which are implemented from both government and developer side. New lucrative schemes from government and advance

research works facilities from AHEC-IIT Roorkee like premier institution are dedicated to encourage the small hydro power developers.

1.2.4 Hydro Turbines and Their Classification

Hydro turbine is a type of prime mover, which converts potential energy of water to shaft power. The turbine shaft coupled with electric generator runs the rotor coil. Thus the electric generator extracts electric energy. The hydro turbines are broadly classified into two categories according to their interaction with water, impulse turbine and reaction turbine. There are many other ways to classify hydro turbines viz. according to their head, shown in Fig 1.4, specific speed, shaft orientation, types of regulation, design concept etc. The classifications are given in the Table 1.5.

Table 1.5: Classification of hydro turbine

Shaft Orientation	**Horizontal Axis**	**Specific Speed**		
	Vertical Axis			
Head		High	Medium	Low
Impulse (Tangential)		Pelton, Turgo.	Cross-flow, Turgo.	Turgo.
Reaction	**Axial flow**		Propeller, Kaplan.	Bulb, Stream, Straflo.
	Radial flow	Francis, PAT.	Francis.	
	Mix flow	Modern Francis.	Modern Francis.	

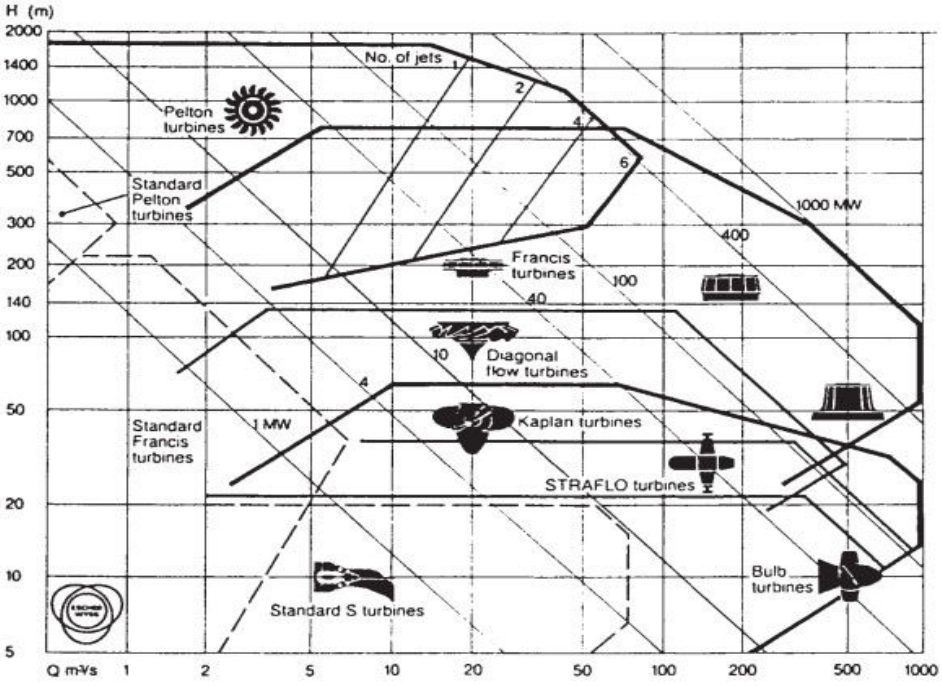

Fig 1.4 Overview of turbine runner and their operating regimes [7]

1.3 COMPUTATIONAL FLUID DYNAMICS

Computational Fluid Dynamics (CFD) is a branch of advanced fluid mechanics, in which the governing equations of fluid flow are solved through numerical technique under various flow domain with the help of fast computation technique (i.e. in computers). Or it is an approximate solution method of real life problems through computation technique with the help of numerical methods. Historically, CFD methods were first implemented to solve the linearized potential flow equations. Two-dimensional (2D) methods, using conformal transformations of the flow over a cylinder and the flow over an aerofoil were developed in the 1930s. Now in this 21st century, the revolutionary progress of computer processing power has provided us great scopes to solve real time three dimensional flow problems of single phase, two phase and even multi-phase fluid flow over complex bodies.

1.3.1 Application of CFD in Hydraulic Turbine

In this modern era of advanced computing, CFD has become an integrated part of hydro turbine industry. The use of Computational Fluid Dynamics to predict the flow in hydraulic machines has brought a substantial improvements in their hydraulic design. The detailed understanding of water flow, its influence on turbine performance and the prediction as well as prevention of cavitation and all other harmful phenomena can thoroughly be scrutinized with the help of CFD technique. The efficient application of advanced CFD is of huge practical importance, as the design of hydraulic turbines is custom-tailored for each project, which not only improves design aspects but also reduce the performance testing times. Which greatly reduces gestation period of a hydro project. Even there are some evidence of new hydro power plants, where the whole design and performance evaluation of prototype were conducted in CFD environment and the design were directly implemented in power house working prototype, without making any physical test model [8].

1.3.2 Limitations of CFD Approach

Although the wide application of CFD in industrial and R&D areas are well acknowledged, but the deviation of approximate solution from CFD, and experimented or measured data form plant site, shows us improvement areas in CFD methodology. Moreover the deviation of results in CFD with experimented data at off-design condition is more significant or deviant. As the outcome

from CFD analysis is more and more depends upon mesh density, therefore there is always a chance of ambiguity in results in every computation process. For more complex fluid flow phenomena, the complicated flow domain results a hesitation in selection of proper turbulence model. Which as a result needs more advanced hybrid turbulence model, and thus the method appears very costly.

1.3.3 Methodology of CFD Analysis

The basic approach behind solving CFD problem is to solve the fundamental fluid dynamic equations in the given flow domain. The governing equations of fluid dynamics are:

Continuity Equation: Also known as conservation of mass equation in which the mass of fluid is considered as conserved.

$$\nabla . \rho V + \frac{\partial \rho}{\partial t} = 0 \tag{1.1}$$

Navier Stokes Equation: It is a special form of momentum equation or Newton's second law of motion. This equation is considered as the most significant equation after Bernoulli's equation in fluid flow, which predicts the characteristics of flowing fluids and their interaction with other bodies.

$$\rho \frac{Du}{Dt} = \rho g - \nabla P + \mu \nabla^2 u \tag{1.2}$$

Energy Equation: The energy equation is the first law of thermodynamics, which is implemented in fluid flow problem with more specified approach by eliminating unnecessary and trivial factors. The special form of energy equation is Euler's equation, which can be derived from Navier Stokes equation. And the integration of Euler's equation gives us the famous Bernoulli's equation, which is nothing but a special form of 1st law of thermodynamics.

$$Ein - Eout = \frac{dEcv}{dt} \tag{1.3}$$

In common fluid dynamics problem we try to execute the situation with continuity equation and momentum equation. In certain cases where the energy exchange happens between control volume and surroundings, we imply energy equation.

The following steps are commonly followed to execute any computational fluid dynamic problem:

(i) Creating flow domain with the help of CAD software.

(ii) Discretizing the flow domain and defining boundary condition.

(iii)Solving the governing equations in discretized flow domain.

(iv)Finally compare computed result with laboratory tested result.

A flow chart has been shown in the Fig 1.5 for better understanding of CFD methodology.

Discretized flow domain are commonly of two types:

(a) Structured grid. (b) Unstructured grid.

The structured grid can be of **O** and **C** type. On the other hand unstructured grid can be triangular or quadrilateral for 2D geometry and tetrahedral or hexahedral for 3D geometry. Grids can be orthogonal (lines meet $\perp$) or non-orthogonal (lines meet other than 90°). Unstructured grids are suitable for complex geometry.

The discretization process can be performed in several methods:

(1) Finite Difference Method (FDM).

(2) Finite Volume Method (FVM).

(3) Finite Element Method (FEM).

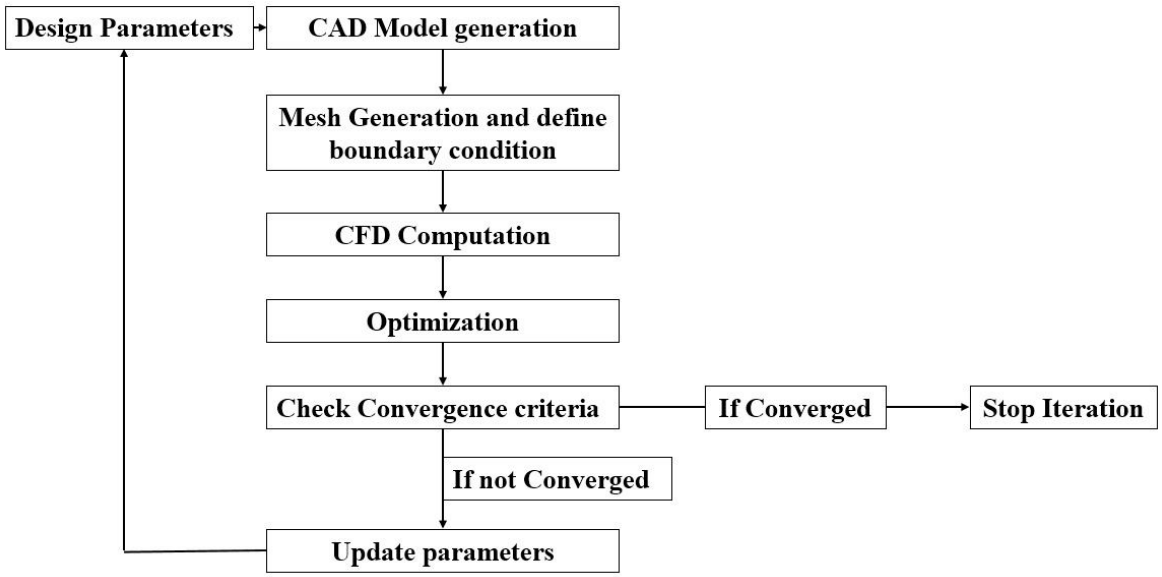

Fig 1.5 Block diagram for CFD based solving methodology of a fluid flow problem

The solving process of given flow problem dependent upon the condition of flow domain. In the laminar regime, the flow phenomena in this region can be analyzed by solving the steady-state Navier-Stokes equations. As per concern of hydraulic turbine the flow domain is inherently turbulent. Therefore the flow in hydro turbine can never be predicted accurately with one particular equation, rather with a set of equations. For different frequency of turbulence there require different turbulence model to predict the nature of flow. Therefore choosing particular turbulence model for certain problem is an important one.

1.3.4 Turbulence and turbulence models

Turbulence can be defined as a behavior of fluid flow, when the Reynold's number goes beyond its critical value. In a broad scale the behavior of a fluid is of two type, laminar and turbulent. To distinguish the nature of a flow Reynolds number is generally used. According to the definition of Reynold's number, it's a dimension less parameter which is a ratio between inertia force and viscous force.

$$Re = \frac{\rho V D}{\mu} \tag{1.4}$$

In laminar flow the viscous force is predominant and therefore it dampens out the perturbation created by inertia force on a fluid particle, where as in turbulent flow the inertia force is predominant. In laminar condition the flow becomes steady and smooth. On the other hand in turbulent flow the nature of flow is unsteady and unpredictable. As turbulent flow inherently complex and unpredictable in nature, there are various attempts have been made throughout history by famous mathematicians, physicists and engineers to model a proper turbulence model to define and approximate the behavior of a turbulent flow. Prandtl mixing length, Reynold averaged Navier Stokes model, Kolmogorov scale are some of the various famous models in turbulence modelling.

According to FLUENT database, FLUENT provides various types of turbulence methods. All are indexed below.

- κ-ε Turbulence model
- κ-ω Turbulence model
- Scale Adaptive Simulation (SAS)
- Detached Eddy Simulation (DES)
- Large Eddy Simulation (LES)

- Wall Modelled LES (WMLES)
- Embedded and Zonal LES
- Other RANS LES Hybrid

Mathematical equations of the few significant and relevant models of turbulence are discussed below:

Reynold averaged model

Here in Reynold averaged model the velocity of fluid particle is considered to have two components one is mean and other is fluctuating. Similarly scalar quantities also have two components.

$$Ui = \bar{U}i + \acute{U}i \tag{1.5}$$

The time averaged form of continuity equation and momentum equation are given below:

Continuity equation

$$\frac{\partial \rho}{\partial t} + \frac{\partial (\rho Ui)}{\partial xi} = 0 \tag{1.6}$$

Momentum equation

$$\frac{\partial \rho Ui}{\partial t} + \frac{\partial (\rho UiUj)}{\partial xj} = -\frac{\partial P}{\partial xi} + \frac{\partial}{\partial xj}\left[\mu \frac{\partial Ui}{\partial xj} + \frac{\partial Uj}{\partial xi} - \frac{2}{3}\delta ij \frac{\partial Ul}{\partial xl}\right] + \frac{\partial}{\partial xj}(-\overline{\acute{U}i\acute{U}j}) \tag{1.7}$$

Filtered Navier-Stokes Model

This model are commonly employed in large eddy simulation problem. In this method a filter function eliminates small eddy formation from the model and applies time dependent Navier-Stokes equation. Filtered form of the continuity and momentum equation are given below:

Continuity equation

$$\frac{\partial \rho}{\partial t} + \frac{\partial}{\partial xi}(\rho \bar{U}i) = 0 \tag{1.8}$$

Momentum equation

$$\frac{\partial}{\partial t}(\rho \bar{U}i) + \frac{\partial}{\partial xj}(\rho \bar{U}i\bar{U}j) = \frac{\partial}{\partial xj}(\sigma ij) - \frac{\partial \bar{P}}{\partial xi} - \frac{\partial \tau ij}{\partial xj} \tag{1.9}$$

Where $\sigma ij \equiv \left[\mu\left(\frac{\partial \overline{U}i}{\partial xj} + \frac{\partial \overline{U}j}{\partial xi}\right)\right] - \frac{2}{3}\mu\frac{\partial \overline{U}l}{\partial xl}\delta ij$ (1.10)

κ-ε RNG

The most widely used closure model is two equation κ-ε model. Although κ-ε turbulence model is very popular to predict the complex nature of swirl flow but it greatly depend upon the wall function and it frequently unable to capture the recirculation in flow. To eliminate this problem, there are several improved version of κ-ε turbulence model has been designed. One such model is κ-ε RNG turbulence model.

$\nu_t = C\mu\frac{\kappa^2}{\varepsilon}$ (1.11)

$\frac{\partial k}{\partial t} + \overline{u}j\frac{\partial k}{\partial xj} = \frac{\partial}{\partial xj}\left[\left(\nu + \frac{\nu t}{\sigma ku}\right)\frac{\partial k}{\partial xj}\right] + Pk - \varepsilon$ (1.12)

$\frac{\partial \varepsilon}{\partial t} + \overline{u}j\frac{\partial \varepsilon}{\partial xj} = \frac{\partial}{\partial xj}\left[\left(\nu + \frac{\nu t}{\sigma \varepsilon u}\right)\frac{\partial \varepsilon}{\partial xj}\right] + C\varepsilon 1 Pk\frac{\varepsilon}{k} - C\varepsilon 2\frac{\varepsilon^2}{\kappa}$ (1.13)

Where $C\varepsilon 2 = C2\varepsilon + \frac{C\mu\eta^3(1-\eta/\eta 0)}{1+\beta\eta^3}$ (1.14)

$\eta = S\frac{\kappa}{\varepsilon}$ (1.15)

$Pk = \nu_t S^2$ (1.16)

$S = \sqrt{2SijSij}$ (1.17)

$Sij = \frac{1}{2}\left(\frac{\partial \overline{ui}}{\partial xj} + \frac{\partial \overline{u}j}{\partial xi}\right)$ (1.18)

κ-ω SST

κ-ω SST or κ-ω shear stress transport model is quite a newer and highly flexible model. In newer days this model is very popular in turbomachinery. It uses modified version of κ-ε turbulence model far from wall and uses κ-ω model near to the wall domain by combining the advantages from both the models.

$\nu_t = \frac{a1k}{\max(a1\omega, SF)}$ (1.19)

$\frac{\partial k}{\partial t} + \overline{u}j\frac{\partial k}{\partial xj} = \frac{\partial}{\partial xj}\left[\left(\nu + \frac{\nu t}{\sigma k}\right)\frac{\partial k}{\partial xj}\right] + Pk - \beta\kappa\omega$ (1.20)

$$\frac{\partial \omega}{\partial t} + \overline{u}j\frac{\partial \omega}{\partial xj} = \frac{\partial}{\partial xj}\left[\left(\nu + \frac{\nu t}{\sigma\omega}\right)\frac{\partial \omega}{\partial xj}\right] + \frac{\gamma}{\nu t}Pk - \beta\omega^{2} + \frac{\sigma\omega}{\omega}\frac{\partial k}{\partial xj}\frac{\partial \omega}{\partial xj} \quad (1.21)$$

1.4 LITERATURE REVIEW

The history of water-wheel for various purpose from extraction of mechanical work to water lifting is of 1000 years old. The application of hydraulic turbine in electricity generation is also an old process. But all process were in efficient due to lack of technology. James B. Francis from Lowell, Massachusetts is the first person who developed the efficient turbine, known as Francis turbine, named after him, in the year of 1850s. The modern impulse hydro turbine was developed by an US inventor Lester Allan Pelton in the year of 1870s. And the axial turbine was invented by Austrian engineer Viktor Kaplan in 1913, which provides wide range of efficient operation due to its adjustable guide vanes and blades. As per efficiency and design concern, the improvement of hydro turbine design is the prime goal of engineers and researchers, since the invention of hydro turbine. And implementation of CFD in this field has not only broadened the scope but also helped to investigate the extremely complex flow phenomena in a thorough manner. Moreover the CFD approach to solve the complex flow phenomena through Francis turbine is economical and time efficient. Although CFD technique is an approximate approach, but its versatility and satisfactory results brought it to the prime research area in hydro turbine industry. In this study the performance prediction of Francis turbine investigated by researchers under various operating condition has been discussed, and the identified gaps in the investigation process has been reviewed.

1.4.1 Justification of CFD analysis in Francis Turbine

Manoj K Shukla et al [9] worked on flow simulation of horizontal axis Francis turbine to validate and correlate the CFD simulation with experimented results. They conducted their research work on prototype model of a Francis turbine of 3.14MW capacity. They achieved almost equal maximum efficiency at the same discharge regime. Their research work validates the flow simulation approach with experimented data and they focused on the modification of casing tip, to make smooth entrance, which improves the efficiency slightly. They have compared the head vs discharge and efficiency vs discharge between experimental value and CFD value, throughout the whole operating range.

Kiran Patel et al [10] published research work on development of Francis turbine using CFD to enquire and validate the flow phenomena. They conducted their experiment in full operating

range from 25% to 130% of loading. They had done a comparison study of losses in different section of turbine under head loss vs loading. Their work clearly showed the flow separation zone in draft tube at 25% and 100% load condition. Their work also showed the pressure distribution on different section of turbine runner under different loading condition. Their paper also covered significance of cavitation and its affected zone.

Santiago Lain et al [11] conducted numerical investigation of a Francis turbine model and compared their result with laboratory prototype to validate their experiment. They performed CFD analysis to draw hill chart of their CAD model and visualize rotor-stator interaction. To draw hill chart they worked with dimensionless parameters viz. discharge coefficient $\varphi = \frac{Q}{\pi\omega R^3}$ and energy coefficient $\psi = \frac{2E}{\omega^2 R^2}$ and conducted five different volumetric flow simulation under certain gate opening condition. Hill chart was plotted between normalized discharge coefficient (along x axis) and normalized energy coefficient (along y axis) to validate the numerically calculated hill chart with actual hill chart. They also conducted calculation of pressure coefficient $C_p = \frac{P - \acute{P}}{\frac{1}{2}\rho U^2}$ to measure pressure in frequency domain in order to investigate unsteady hydraulic phenomenon such as vortex rope and rotor stator interaction. Their results had good agreement with experimented data and they observed, less than 5% deviation of amplitude between both signals.

HU Ying et al [12] conducted an unsteady turbulent flow simulation through a Francis turbine model to investigate pressure and velocity contour in different section of a turbine model. They adopted wall function of no slip condition near the solid wall. They had conducted an elaborate investigation of viscous flow analysis using RNG κ-ε turbulence model to optimize hydraulic design. They also conducted velocity and pressure distribution on optimized model to represent the improvement of efficiency. Their experiment not only advocates the design optimization but also shows the advantage of CFD analysis, because of its time and model efficient activity.

Ruchi Khare and Vishnu Prasad [13] carried out research work on mixing flow in Francis turbine daft tube. Their extensive work on grid sensitivity of Francis turbine efficiency with respect to number of nodes, shows that, initially the efficiency of turbine increases with increase in number of nodes and reaches up to certain point where the efficiency no longer increase with increase in number of grid point. They also showed the efficiency variation of daft tube under different guide vane opening position throughout its entire operational range. They also illustrated the variation

of loss factor of draft tube with respect to speed factor under different guide vane opening condition. They firmly concluded that the whiling and meridional component of velocity vector after exit from runner is greatly influenced by turbine operation regime. It is also observed that these velocity components affects the energy recovery process by draft tube. Although the energy recovery process increases up to certain speed factor but after that it decreases. The paper also shows the variation of daft tube loss with respect to efficiency, under different guide vane opening condition has parabolic correlation.

Fatma Ayancik et al [14] conducted a CFD based design process of Francis turbine. They worked for a horizontal shaft Francis turbine of 2.3MW capacity. They performed their research work on variation of pressure and velocity field in different section of turbine. The optimization process of runner blade profile, stay vane, guide vane and draft tube gave them the overall efficiency up to as high as 92.3%.

Suthep Kaewnai et al [15] conducted CFD based experiments on improvement of Francis turbine. Their challenging work on improvement of turbine model without experimental validation showed that, their new design model was 7% more efficient than existing working model. When the working model was replaced with newly designed Francis turbine model with expected efficiency of 90%, the new turbine model worked more efficiently. Although the improved model achieved efficiency increment by 5% (not as 7%) but the improvement was satisfactory than the previous model.

H W Oh and E S Yoon [16] published research work on flow analysis of inward flow reaction turbine. They concluded that although the pressure loading in turbine blades are performed statically, but the loaded velocity distribution can be substantially affected by dynamic flow condition and blade geometry.

Zoran CARIJA et al [17] conducted flow simulation work on a working prototype model of a Francis turbine of 20MW to validate the CFD analysis. They performed their onsite measurement technique according to IEC-41 international field acceptance standard and simultaneously they investigated virtual flow simulation through κ-ε turbulence model. Their research paper shows the maximum deviation of efficiency (2.89%) happens at 80% gate opening condition and the discharge vs efficiency curve almost agrees each other with negligible deviation in rated condition. The deviation becomes more prominent at higher gate opening condition.

B Firoozabadi et al [18] conducted CFD analysis to investigate the performance of Francis turbine under different blade geometry. In their paper they had shown the optimal turbine model can be selected according to the desirable performance of runner which takes least computational effort. Their paper also focused on the cavitation phenomenon, which explains that the cavitation can be predominately observed in the suction side of runner blade.

1.4.2 Comparison of Different Turbulence Model

Timo Krappel et al [19] conducted flow simulation study to investigate the pert load instability of Francis turbine using different turbulent model. Their study was to reach a quantitatively better numerical prediction of the flow at part load condition and to compute the adequate numerical depth with respect to effort and advantage. As standard practice, their simulation results were as per the steady state approach with SST turbulence modelling. Those results were oriented with transient simulations accompanied with a SST and a SAS (Scale Adaptive Simulation) turbulence model. The structure of the SAS model is in such a manner that it is able to predict the turbulent flow behavior in more detail way. The steady state simulation approach with SST turbulence model overestimates the total losses for the complete turbine, especially in the runner and draft tube by more than 4 % of total head compared with the reference simulation SAS-SST 40M. By using a URANS approach, the deviation is reduced to about 1 %. As the 16M mesh already has a quite good resolution for predicting the large structures of the vortex rope, the losses are quite similar compared to the reference. Generally, the largest deviations of losses can be found in the runner and draft tube domain, where transient phenomena are most dominant.

Dragica Jošt et al [20] conducted an experiment to improvement of efficiency prediction for a Kaplan turbine with advanced turbulence models**.** Their study on ANSYS CFX, projected an overall idea of understanding about different turbulence models like RANS k-ω, k-ε, Baseline (BSL) k-ω, and scale resolving simulation (SRS) models like SAS-SST and LES model. The SAS SST turbulence model is also known as second generation URANS model, as per classification of turbulence models. The model is nothing but the SST turbulence model with an additional term Scale Adaptive Simulation in the ω transport equation. Their investigation showed that the calculated efficiency differ mostly due to different values of flow energy losses in the draft tube and different values of torque in turbine shaft. The efficiency value calculated from steady-state solution with SST was 4.42% smaller than the laboratory measured one. With transient analysis a

significant improvement in result was found. With SST and SAS the efficiency values were smaller than the measured ones by 1.01 and 0.24%. The agreement between measured and numerical values is excellent for SAS and LES, where the discrepancy is 0.09 and 0.05%, respectively. Based on the results it can be concluded that the SAS and LES models are very suitable for flow simulation at operating points with large discharge.

A D' Agostini Neto et al [21] published research work on hybrid RANS-LES turbulence model of draft tube flow. They showed in their paper that, although RANS model, which is based on Navier-Stokes equation, gives good approximation of flow structure under full load and part load operation, but for better approximation LES model can also be implemented although with high computational cost. The hybrid RANS-LES model provides an acceptable balance between computational cost and an improved quality of computational result. Their conducted experiment showed a significant improvement on the velocity profiles for part load condition, which were observed in the SAS-SST calculations. The reduction on the eddy viscosity allows the model to compute smaller eddies. The characteristics and values of the evaluated velocity profiles shows better agreements with the experimental results than the U-RANS approach.

1.4.3 Design Improvement of Francis Turbine Using CFD

Fatma Ayancik et al [14] conducted CFD based design optimization analysis of a Francis turbine model. Their extensive work on 2.3MW hydro project achieved runner efficiency, as high as 97.1% and draft tube efficiency 90% which cumulatively contributed the plant improved efficiency as high as 92.3%.

Suthep Kaewnai et al [15] performed experiment to improvement of Francis turbine prototype using CFD technique. They showed that their improved turbine model is more efficient than the existing turbine model, corresponding to their EGLISU plant. They showed that their model achieved efficiency, more than 7% of existing turbine. And most interesting fact is that they implemented the model in power house without validating the prototype, which awarded excelled efficiency of 5% than existing model.

1.5 OBJECTIVE OF DISSERTATION

Based on the literature review carried out, it has been observed that, various researchers attempted to generate flow model and studied various aspects of performance parameters. Their attempts were to improve efficiency of existing models, defining pressure and velocity variation in various segments of fluid circuit of a hydro turbine. In this dissertation work, an attempt has been made to carry out CFD based performance analysis of a Francis turbine model of an existing hydro power plant with following objectives.

- To develop a model of a Francis turbine in CAD software from existing design parameters.
- To conduct flow simulation of that CAD model in CFD solver.
- To check convergence criteria of CFD simulation with plant measured data.
- Plot graph and tables to validate the CFD model with actual one.
- To compare the results with a typical Francis turbine performance parameters.

1.6 ORGANIZATION OF DISSERTATION WORK

The chapter 1 consists of the relevant information of present energy scenario our country by using a short introduction. A discussion has been drawn on the basis of advantages, disadvantages and state wise potential of small hydro power. An attempt also has been made to define CFD and its various useful aspects in hydro power industry. A summary of research works has been made to accumulate knowledge in the relevant field. And finally the objective of the dissertation work has been shortly discussed.

In chapter 2 a brief introduction has been made on reaction turbines, more specifically on Francis turbine. The behavior i.e. the efficiency, advantages, disadvantages and selection criteria of Francis turbine are been discussed in this section.

Chapter 3 consists of various design parameters and relevant information regarding specified model. The design calculations and methodology are thoroughly discussed in this chapter.

The chapter 4 comprise with a discussion on computation technique in ANSYS on the relevant model which will already been discussed in previous chapter.

In chapter 5 a comparison and validation study has been made on the basis of computed result and collected site data. The velocity and pressure contour in the flowing circuit has also been described. The torque generated in turbine runner under varying flow conditions have also been presented.

In the chapter 6 the conclusions of the present dissertation work and future prospects in the relevant field have been presented.

CHAPTER 2

REACTION TURBINE

2.1 GENERAL

Reaction turbines are the most common type of hydro turbine in which a part of total available head is converted into velocity head and remaining acts as pressure head. In the reaction turbines the working fluid fills the passages completely inside the casing. The pressure or static head of the fluid gradually changes to kinetic energy due to the impulse action between the fluid and the runner. As it has been already shown in the previously mentioned table in chapter one, that reaction turbines are of three types viz. radial, axial and mixed. The most widely operated hydro turbine is Francis turbine, which is a radially inward and axially outward flow reaction type turbine. The modern Francis turbines nature is purely radial inlet flow across stationary guide vanes and flow through the runners are mixed flow type. The tendency from purely radial inward flow device through mixed flow device to near axial flow device increases as specific speed increases. Francis turbine with vertical axis has been shown in the Fig 2.1.

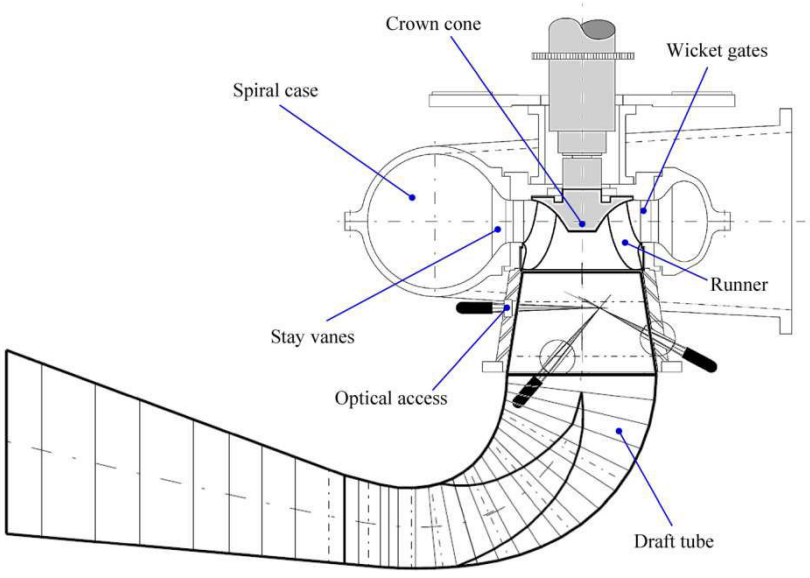

Fig 2.1 Vertical shaft modern Francis turbine and spiral casing [22]

As shown in the above Fig 2.1, a vertical shaft Francis turbine which consists of a spiral casing, stay vanes, guide vanes, draft tube and runner. The spiral case of a Francis turbine is designed in such a way that the velocity distribution towards circumferential direction from the inlet to the stay

vanes is uniformly distributed. The main purpose of the stay vanes are to carry the pressure loads in the spiral case and turbine head cover. Their other purpose is also to converge the flow towards the guide vanes with an optimal gate opening position. The adjustable guide vanes are the only device, employed to control the flow and thus to regulate the power output from a Francis turbine. Leakage through the gaps between the guide vane and facing plate affects turbine efficiency and may cause local erosion. The runner in the Fig 2.2 consists of a crown and band supporting highly curved, three-dimensional sculpted blades. To remove the leakage through the runner and the labyrinth seals which is placed on casing at the crown and band are generally employed. An elbow type draft tube is commonly employed after the runner in downstream.

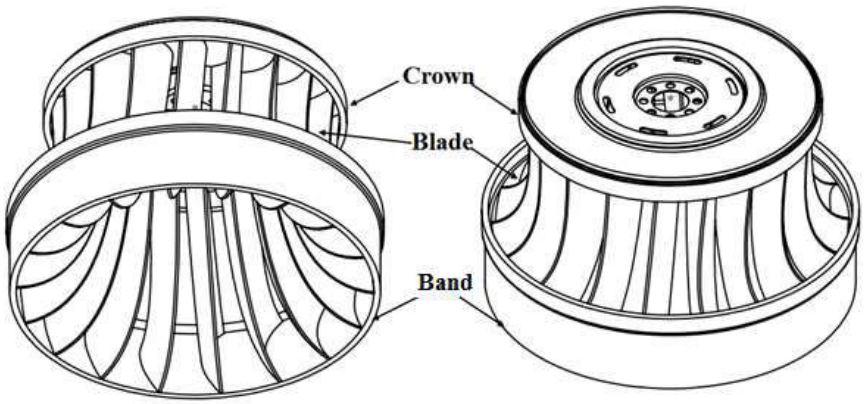

Fig 2.2 CAD visualization of a typical Francis turbine runner

2.2 FRANCIS TURBINE

Francis turbine is a reaction type hydro turbine, where water comes through a penstock flows inside a spiral casing and a series of stay vanes and guide vanes converges the flow of water towards runner vanes. Therefore Francis turbine is a radially inward flow reaction type turbine. Before coming in contact with runner vanes, a part of pressure energy is converted into potential energy. As water flows gradually from inlet to the outlet of runner, a significant pressure variation can be observed. Hence Francis turbines are prone to cavitation. To eliminate cavitation, draft tubes are therefore designed in a diverged conical shape. Various researchers have conducted several experiments to justify the adverse effect of cavitation on performance of reaction turbines. It has been observed from their research work that, at part load operation a vortex rope forms inside draft tubes which not only seriously damages the draft tube wall and runner blades, but also causes

sever noise during operation. In India, the hydro projects bases on Himalayan belt face silt erosion problem. Silt erosion is also an adverse phenomenon occurs due to the local impaction of quartz like strong particles to the runner blades.

2.2.1 Performance of Francis Turbine

It a well-known fact that, hydro turbine is the most efficient prime mover, and among hydro turbines, Francis turbine is the most efficient one. Few commercial Francis turbine can perform as high efficient as 95%. If the guide vane opening angle α_1 and runner vane inlet outlet angle β_1 is known, we can derive the efficiency of Francis turbine runner. The velocity triangle at inlet and outlet of a typical Francis turbine has been shown in the Fig 2.3. Where velocity of jet at inlet and outlet are V_1 and V_2 and velocity of flow at inlet and outlet are V_{f1} and V_{f2} respectively.

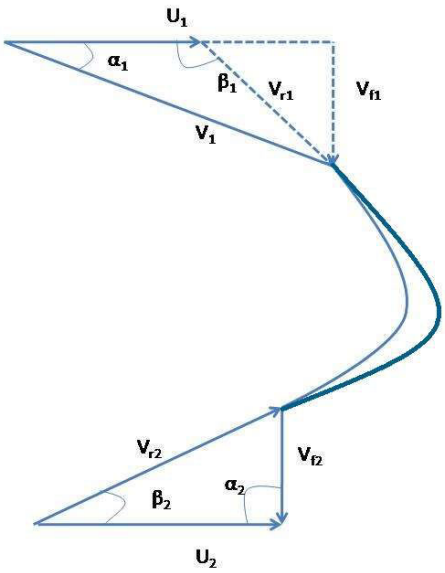

Fig 2.3 Velocity triangle of a Francis turbine runner vane

It can be mathematically shown that work done by a Francis runner per unit second per unit mass is $W = V_{f1}^2\{cot\alpha_1(cot\alpha_1 - cot\beta_1)\}$ (2.1)

Loss of energy $E_1 = \frac{V_{r2}^2}{2} - \frac{V_{r1}^2}{2}$ (2.2)

Overall efficiency $\eta_o = \frac{P}{\rho g H}$ (2.3)

Where P is total power output and H is net head.

2.2.2 Efficiency and Hydraulic Losses

Although Francis turbine is the most efficient turbine, but its part load efficiencies are very poor throughout its working range. Therefore Francis turbines are commonly employed in those power houses where there is no or very little seasonal flow variation observed throughout the year.

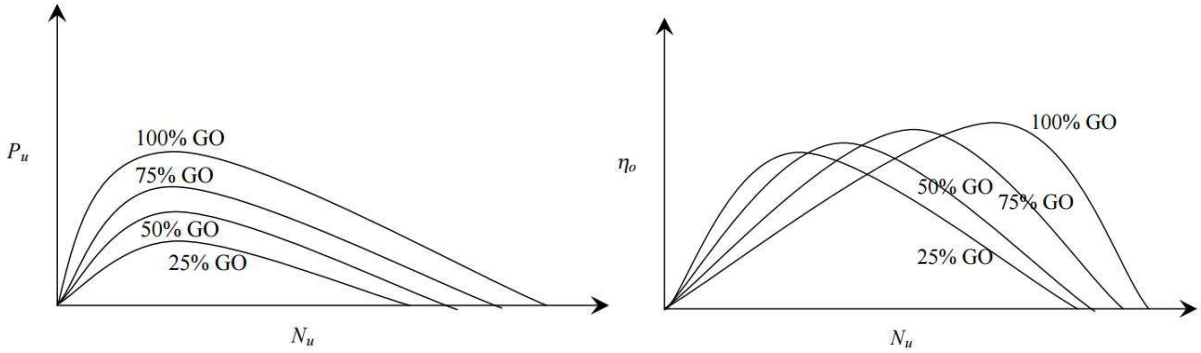

(i) **(ii)**

Fig 2.4 Main characteristic graph of a typical Francis turbine, (i) is the graph between unit power to unit speed under different gate opening position and (ii) is the graph between overall efficiency and unit speed under different gate opening position [23]

It can be observed from the above Fig 2.4 that the best power output and best efficiency can be achieved only at 100% gate opening position. In a hydro power plant the turbine must run the electric generator at a synchronous speed, which is equal to the frequency of grid, where the generator supplies the electricity. The synchronous speed of a hydro turbine can be calculated from the equation below.

$$N=\frac{120f}{p} \tag{2.4}$$

Where N is the synchronous speed of turbine in RPM, f is the frequency of grid in Hz and p is number of poles in generator.

When suddenly the grid fails and the demand of load becomes zero and simultaneously the hydraulic governor fails to perform, the turbine abnormally starts to run at its maximum speed,

this speed is known as runaway speed. At this no load condition and maximum possible speed the turbine must be designed so that it run in its safe limit.

A reaction type turbines like Francis turbine are prone to cavitation. Cavitation is an undesirable phenomenon where the pressure of flowing water at the exit of turbine blade drops below the vapour pressure of water at that temperature. Consequentially the vapour forms bubbles and the vapour bubbles carried to the high pressure zone, where the bubble collapses and cause detrimental effect like local pitting on turbine blade, vibration and noise etc.

To avoid the cavitation, scientist Thoma developed a formula of dimension less coefficient to calculate safe head of operation, which is known as Thoma's cavitation factor σ.

Thoma's cavitation factor $\sigma = \frac{H_a - H_v - H_s}{H}$ (2.5)

Where Ha is atmospheric pressure head, Hv is vapour pressure head, Hs is suction head and H is maximum operating head. The influence of Thoma's cavitation factor on turbine efficiency has been shown in the Fig 2.5.

The critical Thoma's cavitation factor for Francis turbine is $\sigma_c = 0.0432(N_s/100)^2$ (2.6)

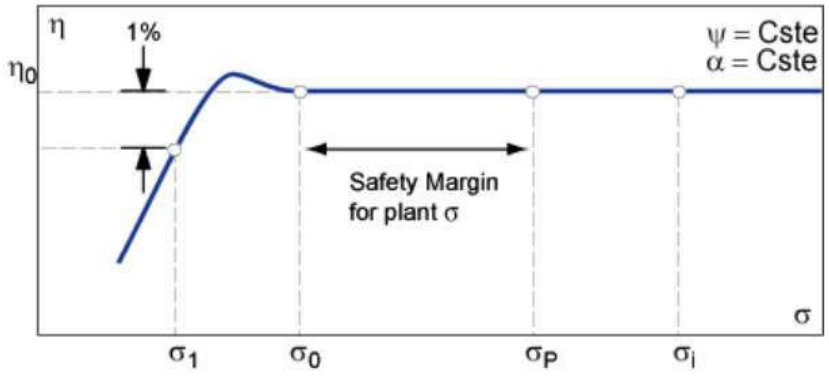

Fig 2.5 Cavitation curve for Francis turbine by keeping specific energy coefficient of turbine constant for a given guide vane opening angle [24]

Where σ_1, σ_0, σ_p are consecutively cavitation factor at 1% drop of efficiency, lowest value of cavitation factor and permissible value of cavitation factor at its working rang. η_0, α, ψ are consecutively the overall efficiency, guide vane opening angle and specific energy coefficient.

Inside a hydraulic turbine, it has been observed that the head losses are highest in draft tube section followed by runner stay vane guide vane and scroll casing, which is shown in the Fig 2.6. Pankaj P. Gohil et al [25] showed in their paper a variation of losses of head in different section of a Francis turbine.

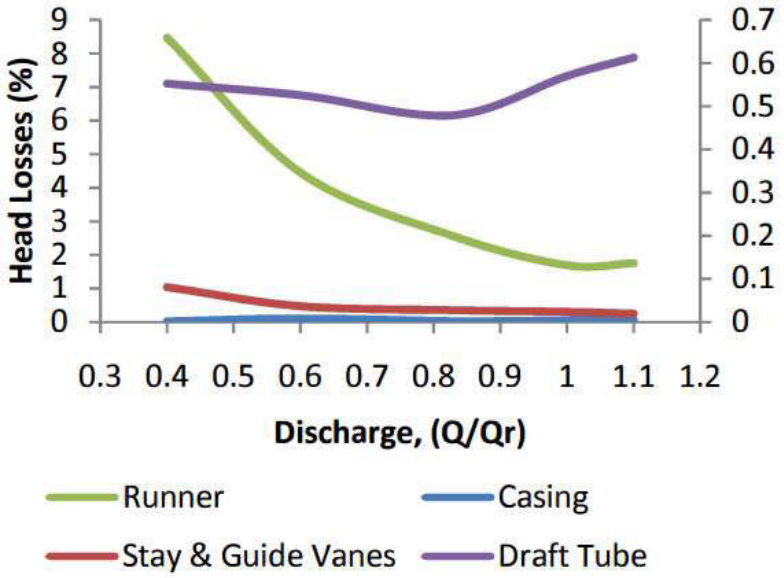

Fig 2.6 Head losses in various section of a Francis turbine against discharge [25]

CHAPTER 3
DESIGN PARAMETERS AND MODELING OF FRANCIS TURBINE

3.1 GENERAL

Francis turbine is the mostly used hydro turbine in the world. It is largely used in large hydro project due to its full load efficiency. It also employed in small hydro projects, where discharge rate is invariant throughout the year. In a power plant turbine is considered as the heart of power house. The complete plant layout is designed on the basis of turbine size. And the turbine size is calculated from the site potential. Therefore choosing appropriate runner diameter for a power house is always the first priority. There are various standards available throughout the world, to estimate the dimensions of different component of a power house on the basis of experience and research work.

3.2 SELECTION OF HYDRO TURBINE PLANT

To carry out the performance evaluation of a Francis turbine, it is an important step to select proper hydro power plant. To model and investigate the turbine setup, a detailed and thorough design data is a prime requirement. Here in this dissertation work, Rajwakti Small Hydro-Electric Plant data has been considered, which is situated in Chamoli District of Uttarakhand. The plant is located at an altitude of 6620 m from mean sea level and at a distance of 196km from Rishikesh. The hydro project is a run-off-river scheme, extracting hydro power from the river Nandakini, a tributary of Alaknanda River and feeds the electricity to 66kV grid provided by Uttarakhand Power Corporation Limited (UPCL).

The specifications for designing is given in the Table 3.1:

Table 3.1: Specifications of Rajwakti SHP Plant

Parameters	Specification
Type of turbine	Horizontal shaft Francis turbine
Potential	4.4MW
Design discharge	10.50 m^3/s
Net head	52m
Annual energy generation	26MU
Turbine maximum efficiency	93.2%
Runner diameter	0.921m
Rotating speed	600 rpm
Specific Speed	218
Number of guide vanes	16
Number of runner blades	13
Maximum guide vane position	40.8°
Minimum guide vane position	0°
Maximum runway speed	1142 rpm
Plant overall efficiency	82.14%
Type of draft tube	Elbow-type

3.3 DESIGN PARAMETERS

Based on the available design data, detailed dimensioning and creating CAD models have been modeled. The main components of the relevant turbine setup are listed below.

i. Casing
ii. Runner
iii. Guide vanes and stay vanes
iv. Draft tube

3.3.1 Casing

The casing of a Francis turbine is an involute type shown in the Fig 3.1. For involute spiral casing the design methodology has been adopted from IS 7418-1991 [26].

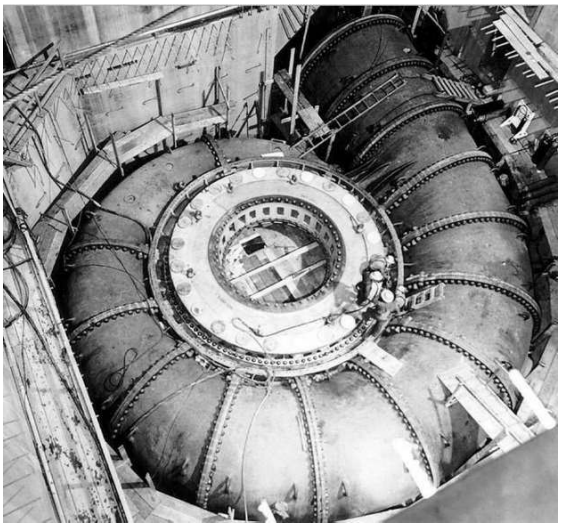

Fig 3.1 Involute casing of Francis turbine [27]

The empirical formulae for designing spiral casing are given below:

Flow through the penstock $Q=V_{penstock}\frac{\pi}{4}D_{penstock}^2$ (3.1)

Radius of casing $R_{casing} = R_{runner}+\frac{\kappa\theta}{2\pi}D_{penstock}$ $0>\theta>=1.89\pi$ (3.2)

Flow per degree through penstock $Q_\theta = Q\frac{\theta}{2\pi}$ (3.3)

Here in this model the involute profile has been divided in to 16 equal segments. The entrance of the spiral casing i.e. the exit of penstock has been considered according to standard assumption. $D_{penstock}=1.45 X D_{runner}$. (3.4)

Therefore, $D_{penstock}=1.45 X 0.921=1.33545m$

To check the permissible limit of penstock diameter, the maximum velocity of water through the penstock is $V_{max}=\frac{4Q}{\pi D_{penstock}^2}$ (3.5)

That is $V_{max}=7.5m/s$. Which is less than maximum limit of 10m/s.

Using the formula 3.2 the radii of different segment of involute casing are been calculated below. The value of κ are commonly considered as unity. The purpose of involute spiral casing is to provide uniform circumferential velocity towards turbine runner.

A=.921+$\frac{22.5}{360}$X1.335=.921m

B=.921+$\frac{45}{360}$X1.335=1.0878m

C=.921+$\frac{67.5}{360}$X1.335=1.1171m

D=.921+$\frac{90}{360}$X1.335=1.2547m

E=.921+$\frac{112.5}{360}$X1.335=1.3382m

F=.921+$\frac{135}{360}$X1.335=1.4216m

G=.921+$\frac{157.5}{360}$X1.335=1.5050m

H=.921+$\frac{180}{360}$X1.335=1.5885m

I=.921+$\frac{202.5}{360}$X1.335=1.672m

J=.921+$\frac{225}{360}$X1.335=1.7553m

K=.921+$\frac{247.5}{360}$X1.335=1.8388m

L=.921+$\frac{270}{360}$X1.335=1.922m

M=.921+$\frac{292.5}{360}$X1.335=2.0056m

N=.921+$\frac{315}{360}$X1.335=2.0891m

P=.921+$\frac{337.5}{360}$X1.335=2.2172m

Q=.921+$\frac{360}{360}$X1.335=2.256m

After tracing the points from A to Q on Solidworks 3-D CAD software, the involute profile is traced with a spline, which is shown in the Fig 3.2 below.

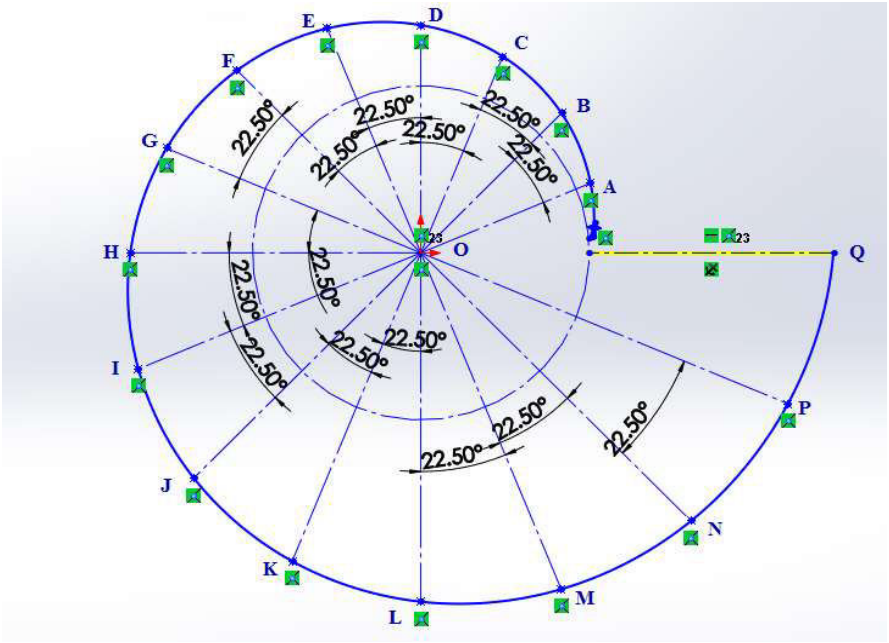

Fig 3.2 Involute profile of spiral casing

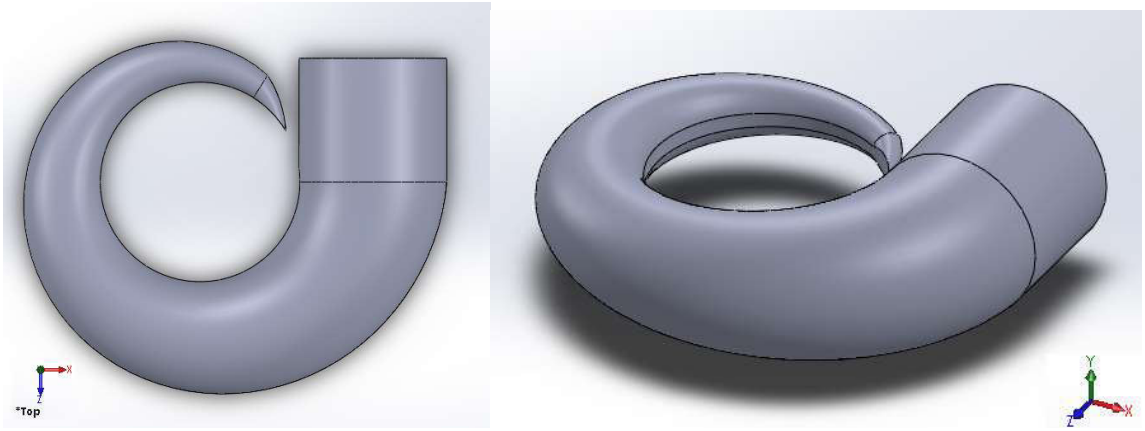

(a) Top View **(b) Isometric View**

Fig 3.3 Top and isometric view of full-scale involute spiral casing

3.3.2 Runner

The most crucial component of a hydro power plant is its turbine. On the basis of runner diameter, dimensioning of every other components are constructed. The basic parameters to construct the full-scale CAD model of runner is given in Table 3.2.

Table 3.2: Runner specifications

Component Name	Specification
Runner diameter	0.921m
Width of runner	0.340m
Crown diameter	0.767m
Runner band height	0.126m
Material	Stainless steel (Cr16-Ni5)
Strength of (Cr16-Ni5)	990N/mm²

The thickness of runner blade is calculated from the formula [28]:

$$t = \sqrt{\frac{2B^2 \Delta P}{\sigma}} \tag{3.6}$$

Where t is thickness of blade, B is B= width of runner. ΔP is maximum pressure difference at the entrance of turbine. σ= yield strength of runner material.

To calculate minimum thickness of runner vanes t_{min}, above mentioned formula $t = \sqrt{\frac{2B^2 \Delta P}{\sigma}}$ can be applied. Where B=0.340m. ΔP=ρ.g.h (where ρ=1000kg/m³, g=9.81m/s² and h=46.65m net head). ΔP=1000*9.81*46.64 = 457.54x10³ N/m².σ= yield strength of SS Cr16-Ni5, which is 990N/mm².

$t = \sqrt{\frac{2*0.340^2*457.54*10^3}{990*1000*1000}}$ = 0.0188m~0.02m.

The blade profile is constructed on the BladeGen®, a blade profile generating tool associated in ANSYS simulation software as shown in the Fig 3.4.

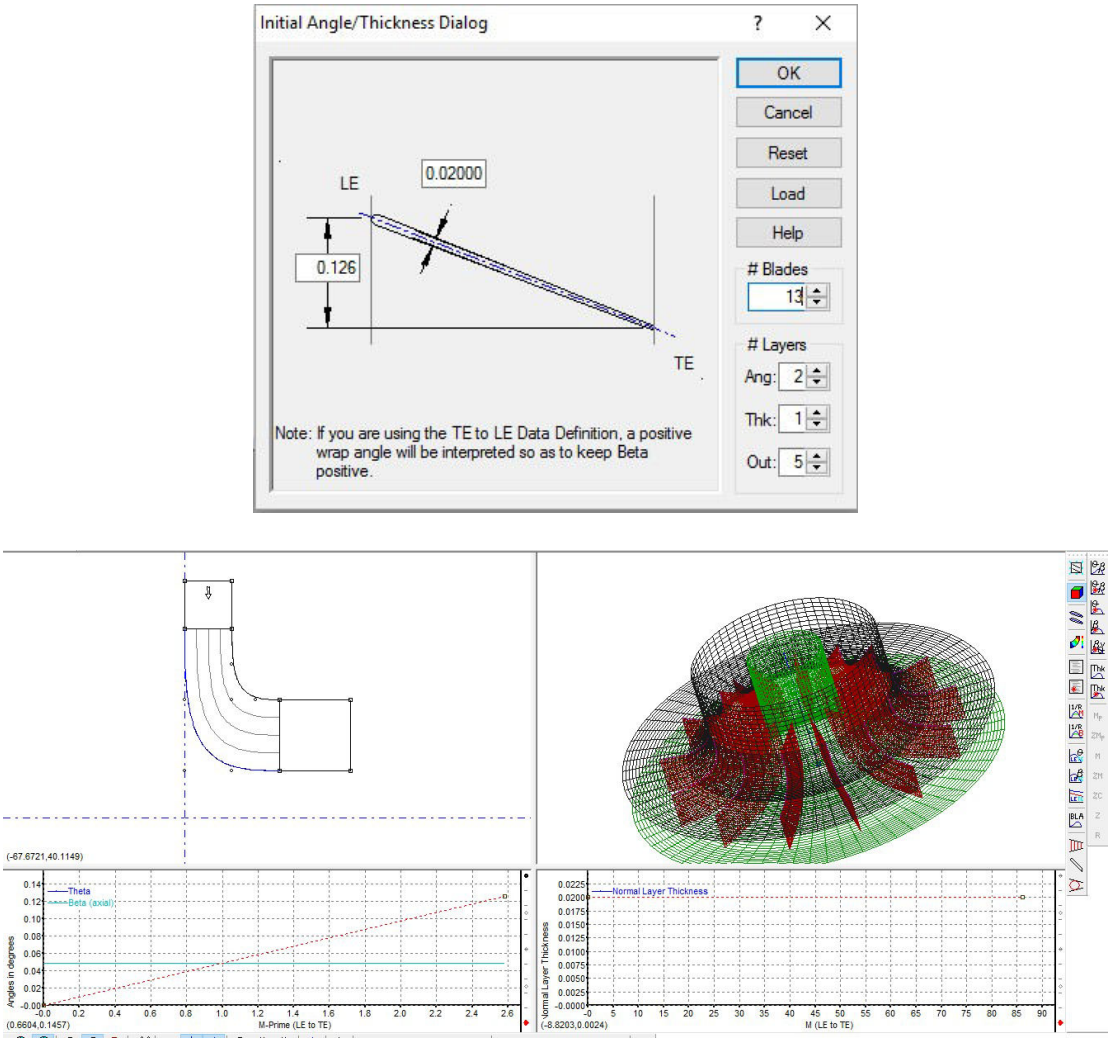

Fig 3.4 Blade profile designed from BladeGen

The designed blade profile is then imported to Solidworks to perform the design of runner.

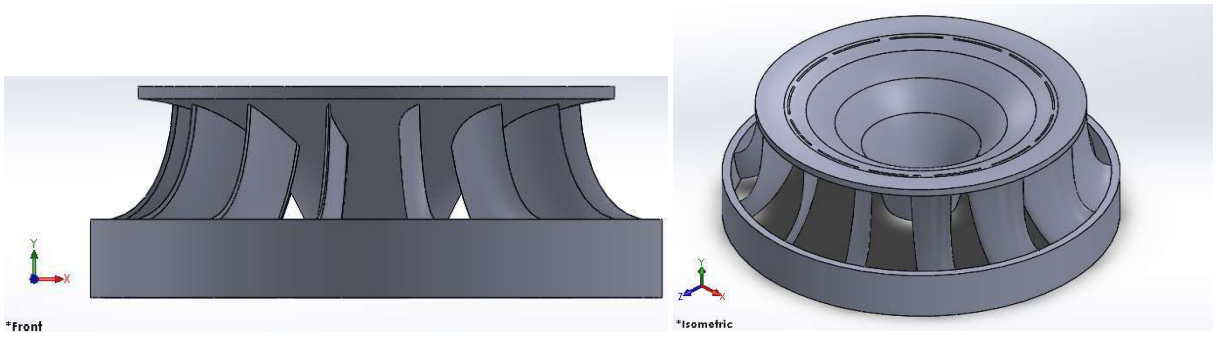

Fig 3.5 Front and isometric view of runner

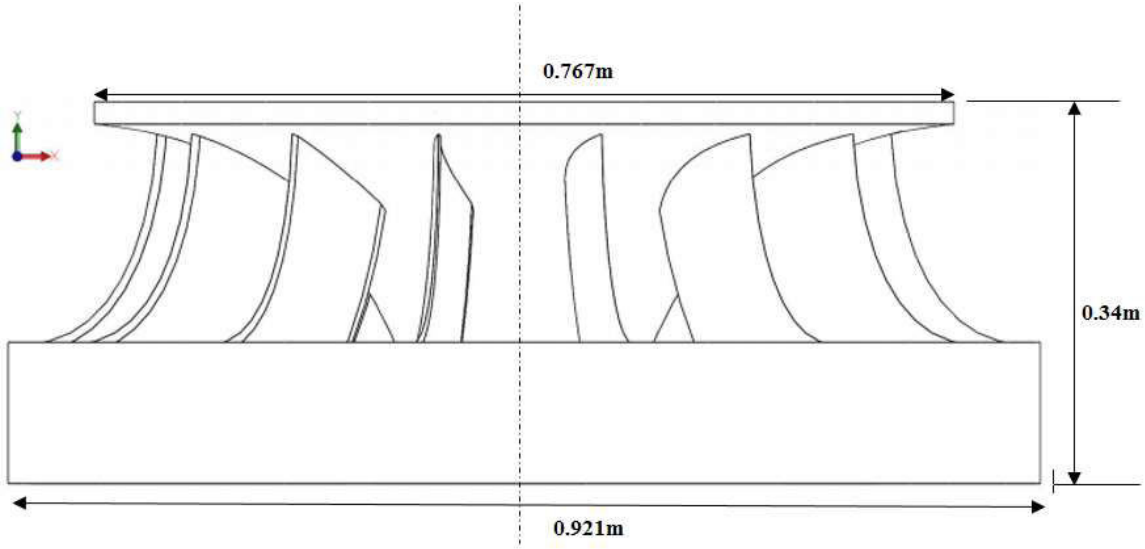

Fig 3.6 2-D sketch with dimension of runner

The full scale turbine solid model has been shown in the Fig 3.5, and 2-D sketch with dimension has been shown in Fig 3.6.

3.3.3 Guide Vanes and Stay Vanes

To design the hydro foil for guide vane and stay vane, standard manual [29] provided by Lulea University of Technology, Sweden has been followed. Blueprints provided by the manual for hydro foil design have been shown consecutively in the Fig 3.7 and 3.8.

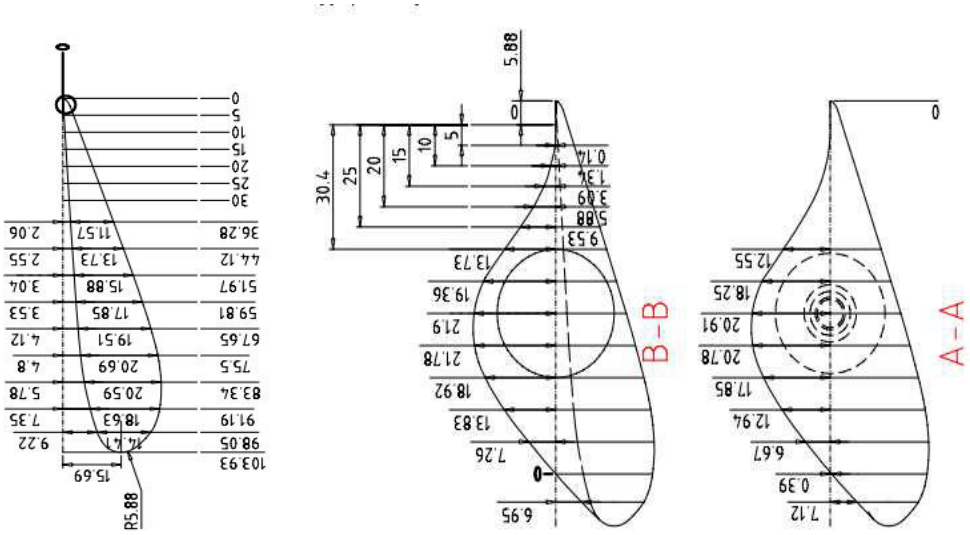

Fig 3.7 Hydro profile for guide vane [29]

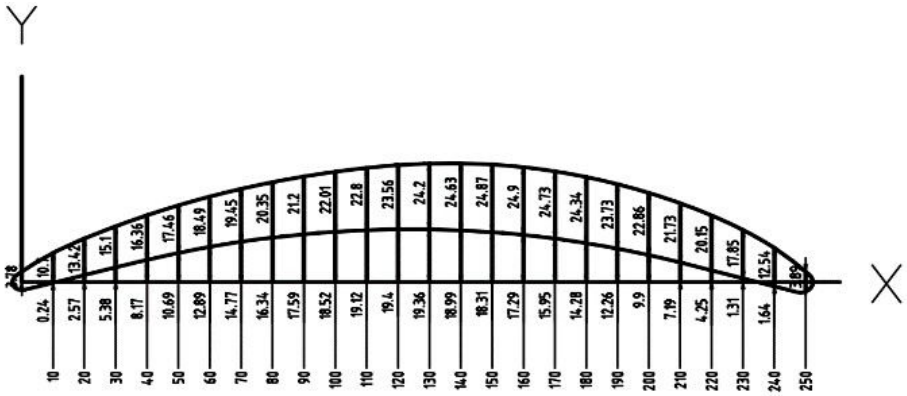

Fig 3.8 Hydro profile for stay vane [29]

The hydro profile for guide vane and stay vane are both drafted in Solidworks and traced with spline with proper dimensions.

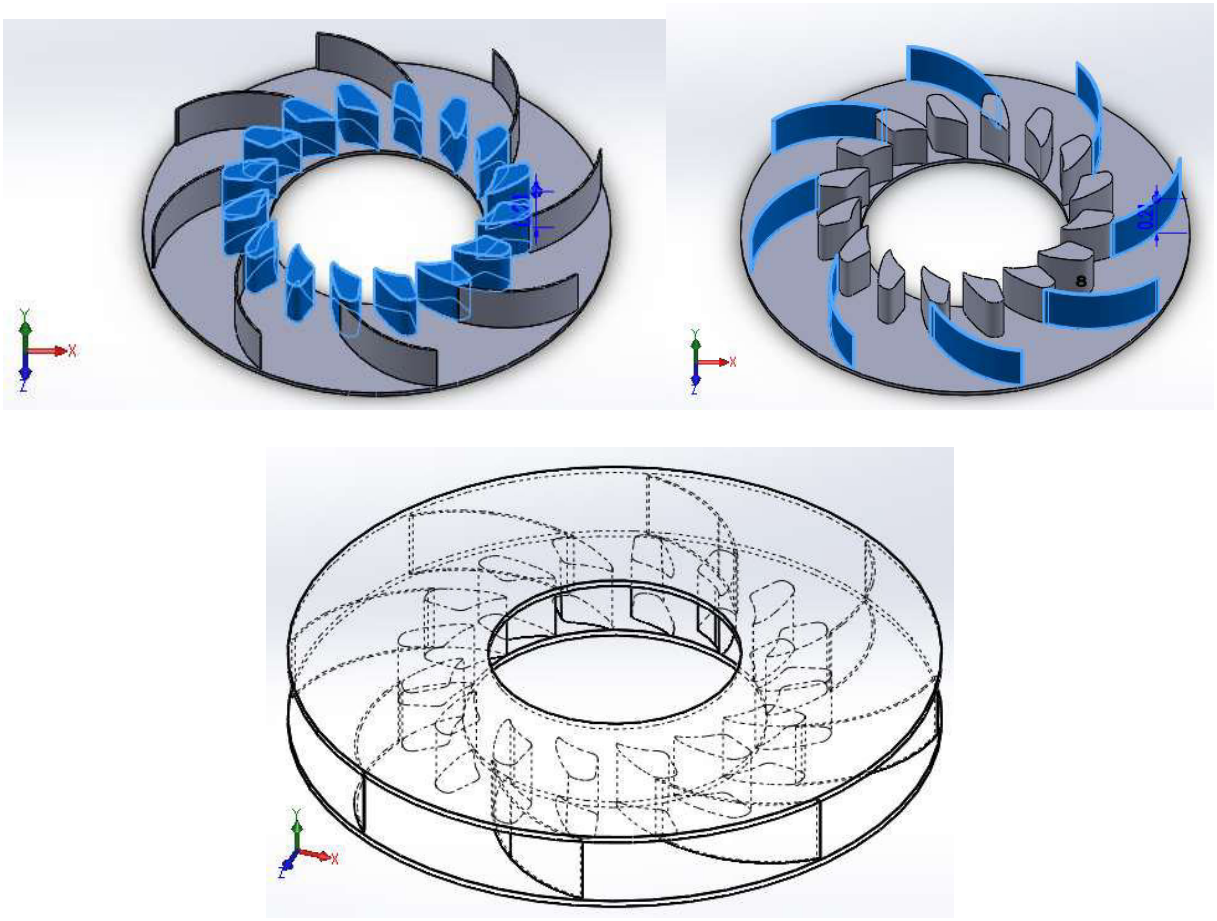

Fig 3.9 Guide vanes and stay vanes inside casing

The above Fig 3.9 represent the full-scale model of guide vanes and stay vanes inside turbine casing. There are sixteen guide vanes and eight stay vanes are assembled inside casing of the turbine model.

3.3.4 Draft Tube

In this design the draft tube is an elbow type in construction. For designing draft tube, IS 5496-1993 [30] has been followed. The entrance is circular and gradually diverges to again circular section.

The given parameters for draft are given in the Table 3.3:

Table: 3.3 Dimension of draft tube

Parameters	Dimension
Draft tube total length	4.60m
Draft tube inlet diameter	0.921m
Draft tube exit diameter	1.784m
Concrete length	16.6m

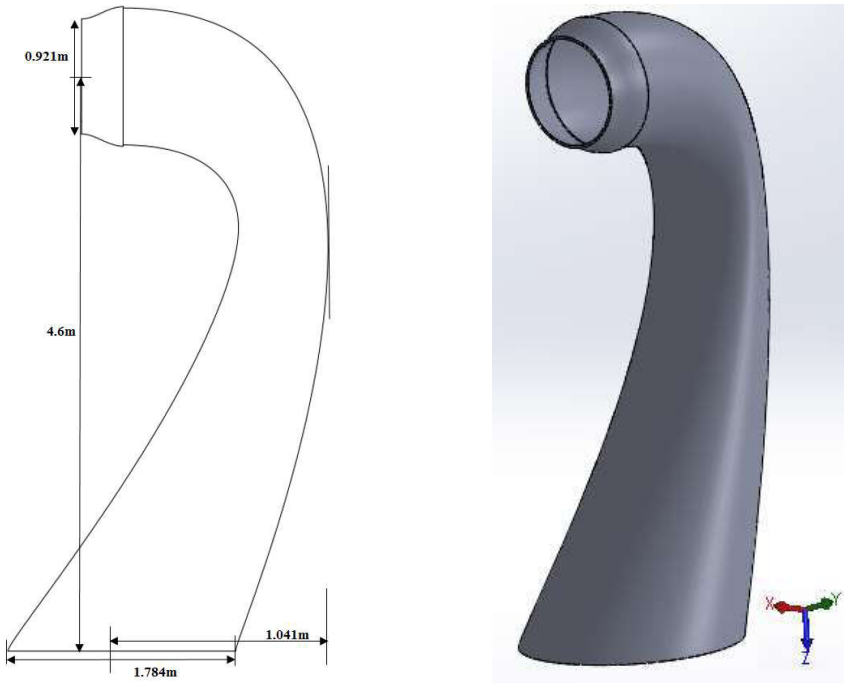

Fig 3.10 2-D and 3-D sketch of draft tube with dimension

After designing the different components in Solidworks, the all part models are assembled in Solidworks assembley design section.The full-scale assembly model of the turbine setup is shown in the Fig 3.11 and 3.12.

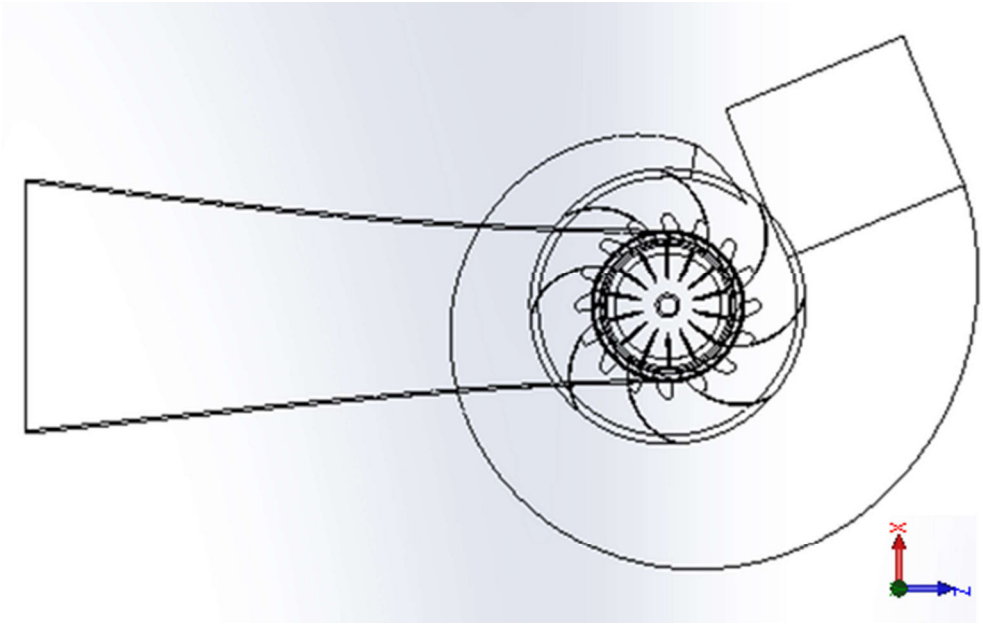

Fig 3.11 Top view of turbine wire-frame assembly model

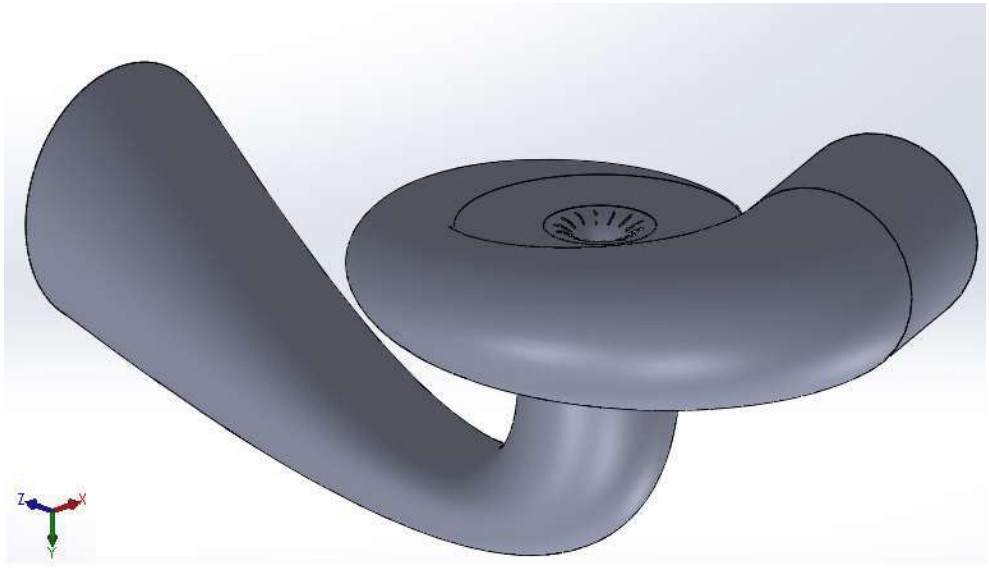

Fig 3.12 Isometric view of Francis turbine assembly model

It is a common practice to convert the assembly file to a standard universal extension file, so that the computational solver can identify the model in its own platform. Here in this work the assembly file is converted to parasolid format. Which features an excellent and minute detailes of the each and every segment of sasembly file. The assembly fie then imported to ANSYS Workbench Design Modeler which is shown in the Fig 3.13.

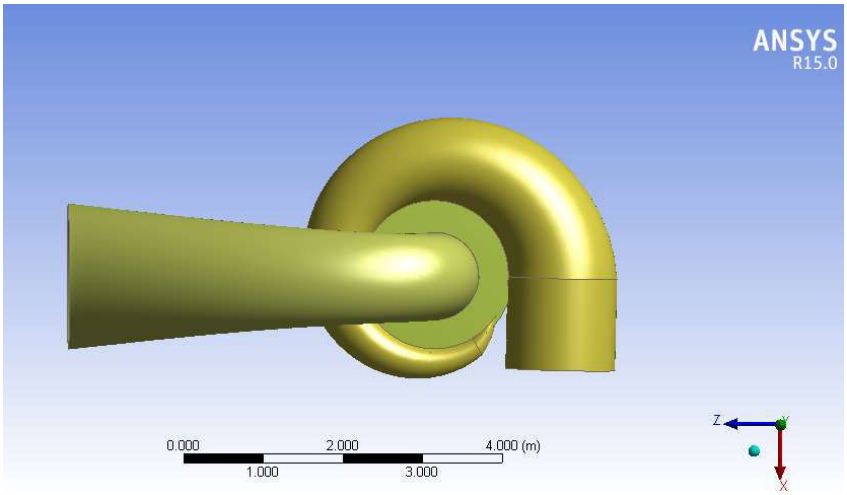

Fig 3.13 Complete assembly moden in ANSYS

CHAPTER 4
NUMERICAL SIMULATION

4.1 GENERAL

Under this chapter 4 the simulation of the Francis turbine setup has been performed and the nature of flow field has been investigated. To run the whole process there are various steps, which are required to be followed. In this chapter the necessary steps and detailed procedure are discussed in subsequent paragraphs. The assembly file constructed and discussed in previous chapter are already viewed and operated under a different perspective. The first step in this simulation work comprise with creation of flow domain. In the later paragraphs deals with selection of boundary name and mesh generation. The mesh structure of each and every components and their corresponding mesh statistics are also discussed with thorough procedure. After carrying out the flow simulation under different flow conditions, the observed results and flow characteristics are discussed in next Chapter.

4.2 CREATION OF FLOW DOMAIN

To conduct the flow simulation of the Francis turbine model, the first and foremost step is to define flow domain. This paragraph describes the detailed procedure to generate flow domain of the whole turbine model.

4.2.1 Import External Geometry

It has already been discussed under previous chapter 3 that, the generated turbine model in Solidworks is needed to be converted into a standard universal file format, so that ANSYS can identify the 3-D geometry of the model. Here, for the simulation purpose the model of assembly file has been exported to PARASOLID format with (.t_x) format. As the performance analysis has been conducted in ANSYS Fluent software, the exported PARASOLID model is needed to be imported to ANSYS Fluent.

The steps corresponding to import geometry and defining flow domain are given below:

- After opening ANSYS Workbench R15, select Fluid Flow (Fluent) from the toolbox on the left side.
- As the Fluent toolbox opens, select the Geometry section. Which will open a new window.

- From the new window of geometry opens, select file menu from the top left corner and click onto the import external geometry.
- After clicking onto the selected option, a panel will open, from where navigate to the library, where the assembly file has been saved.
- Selecting the geometry an import notification will arise in the left panel tree. Then by pressing right click and selecting ‘generate’ option will make the model visible on the graphics window which is shown in the Fig 4.1 and 4.2.

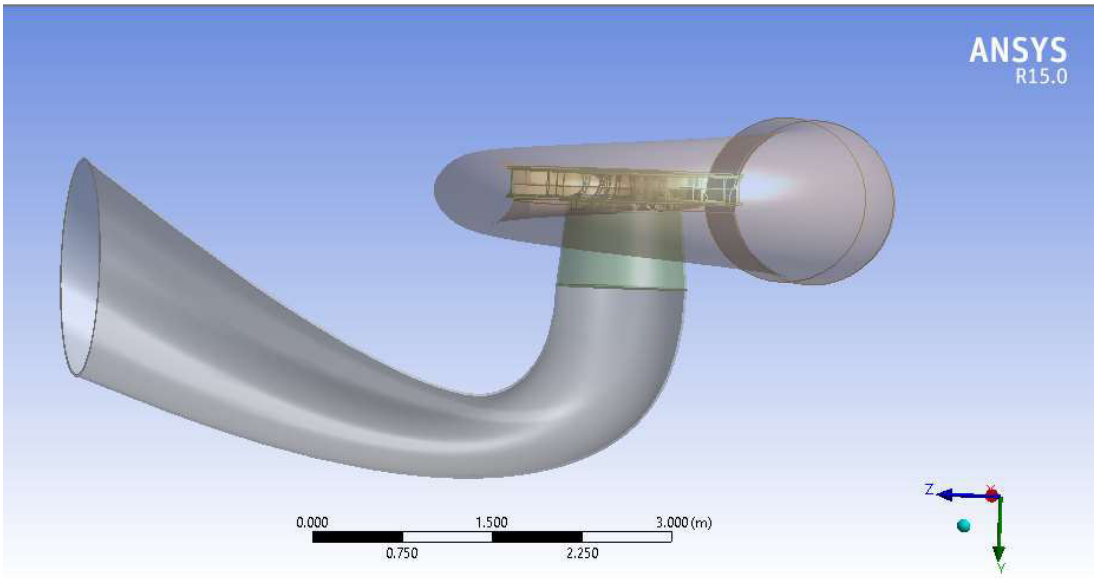

Fig 4.1 Imported Assembly model to DesignModeler in ANSYS

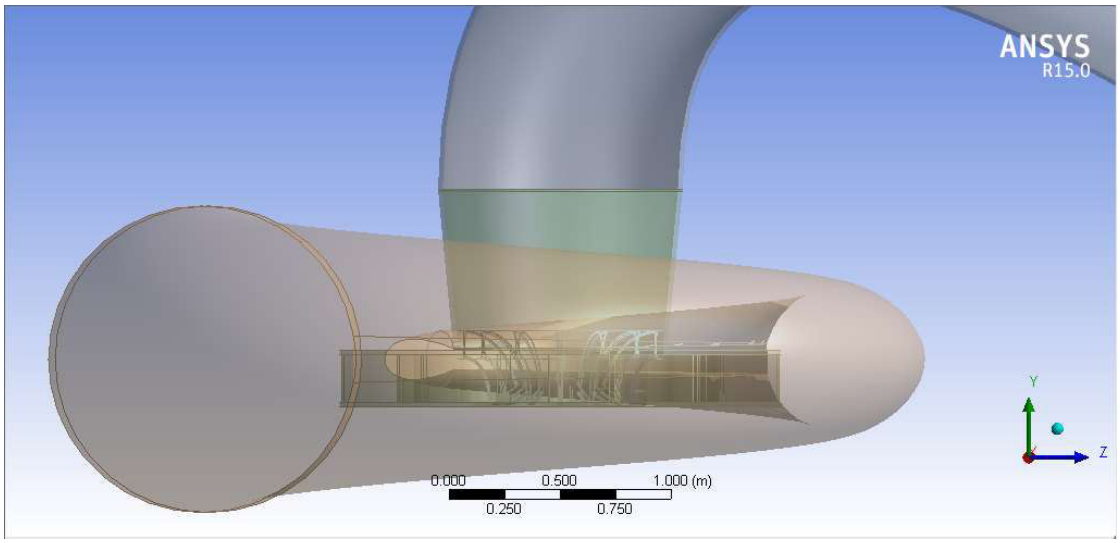

Fig 4.2 Close view of runner inside casing

As the dissertation work is concerned with the performance analysis of Francis turbine, therefore the bulky involute casing has been eliminated from the subsequent study.

The generated new geometry of the turbine setup is shown in the Fig 4.3 and 4.4, which consists with stay vanes, guide vanes, runner and draft tube.

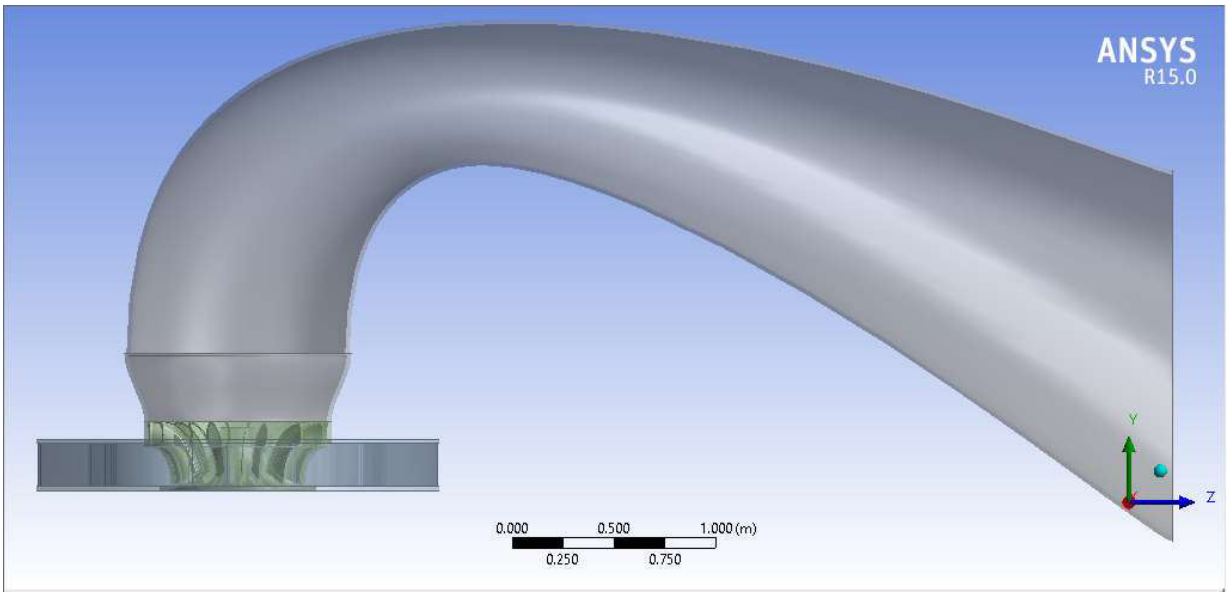

Fig 4.3 Separated assembly model with stay vanes, guide vanes, runner and draft tube

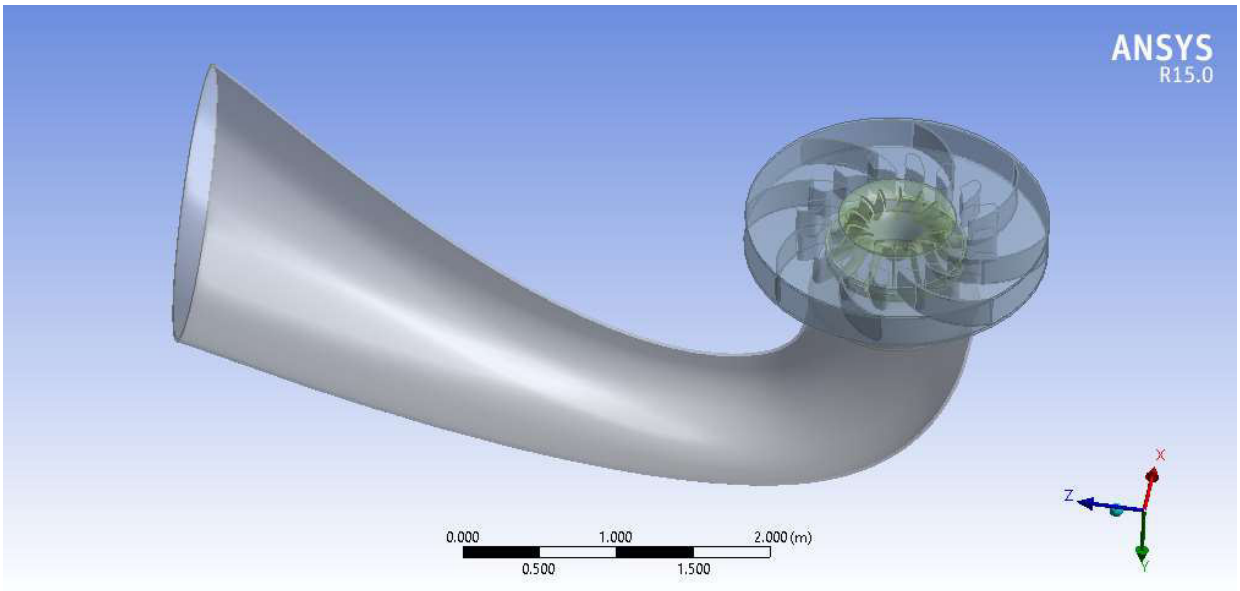

Fig 4.4 an isometric view of turbine setup in DesignModeler

4.2.2 Define Flow Domain

As the assembly model is hollow and open, it is necessary to create a solid boundary inside the cavity. Therefore the following steps are needed to be followed to generate solid boundary.

- To fill the hollow section inside the assembly model, it is necessary to cap the boundaries with surfaces. Therefore the edge at the exit of draft tube and the edge in circular hole of crown is selected simultaneously and the 'surfaces from edges' option is selected from the 'concept' menu. The entrance cylindrical surface before stay vane was already created during solid modeling.
- After capping the whole body with surface select 'fill' option from 'tools' menu. Here the 'extraction type' will be by caps and the target body will be 'selected body'. Then selecting the whole body option will lead to a continuous solid medium inside the cavity.
- After suppressing the different components one by one from the geometry of the assembly, the solid boundary will be visualized in graphics window shown in the Fig 4.5 and 4.6.

Fig 4.5 Flow domain

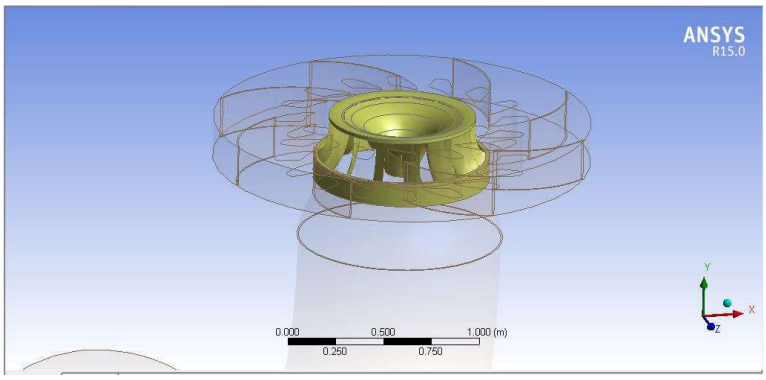

Fig 4.6 Turbine through the wire frame view of flow boundary

4.3 MESH GENERATION AND BOUNDARY SELECTION

Before conducting flow simulation it is an essential step to discretize the flow domain in to various small segments. The main purpose of discretization of flow domain is to create the small segment of elements, so that the governing equation can be solvable numerically on that small domain. The discretization, i.e. mesh generation is so important that it the method of discretization vastly effects on generated results and their level of accuracy. Although it's very time consuming process but in common practice to get higher order accuracy, tetrahedral unstructured fine mesh are commonly adopted. Here in his dissertation work the same process of discretization method has been adopted.

4.3.1 Mesh Generation

The standard methodology to generate mesh in ANSYS-ICEM has been indexed below:

- After finishing the creation of flow domain in the 'Design Modeler' go to fluent mesh option in the first dialogue box.
- In mesh window there will appear a 'Mesh' option in left side tree. By pressing right click and selecting 'Generate Mesh' option will lead to an auto generated mesh structure of the flow domain which is shown in the Fig 4.7, 4.8 and 4.9.
- On the lower left corner of 'details mesh' option the sizing menu allows to modify the 'relevance center' and 'smoothing' options. By changing the relevance center option from coarse to fine and smoothing option from low to high can lead us to generate finer mesh.
- In the 'assembly meshing' option, changing the method from none tetrahedrons will allow us to modify the structure the mesh to all tetrahedral mesh as shown in the Fig 4.10 and 4.11.

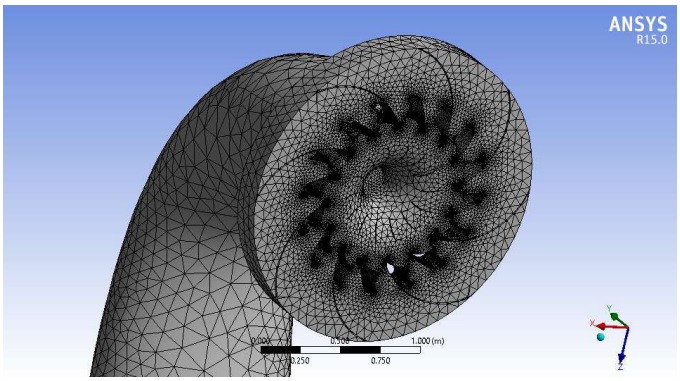

Fig 4.7 Unstructured coarse mesh

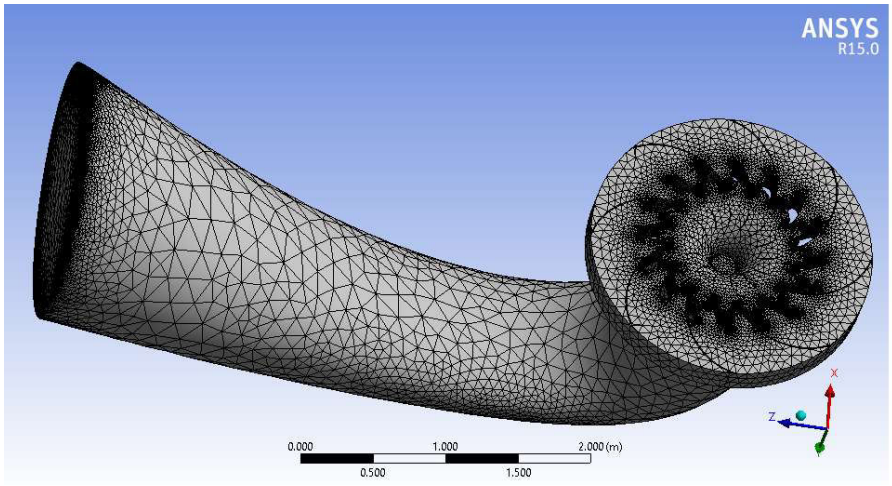

4.8 Coarser mesh of flow domain

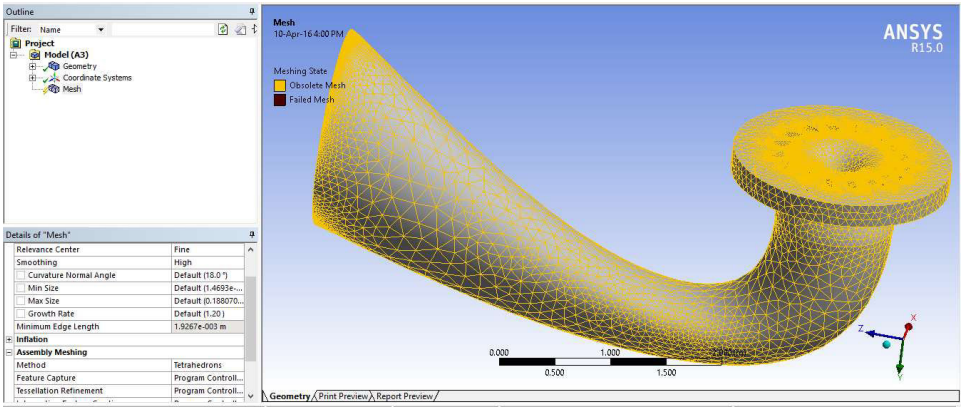

4.9 Flow domain before mesh refinement

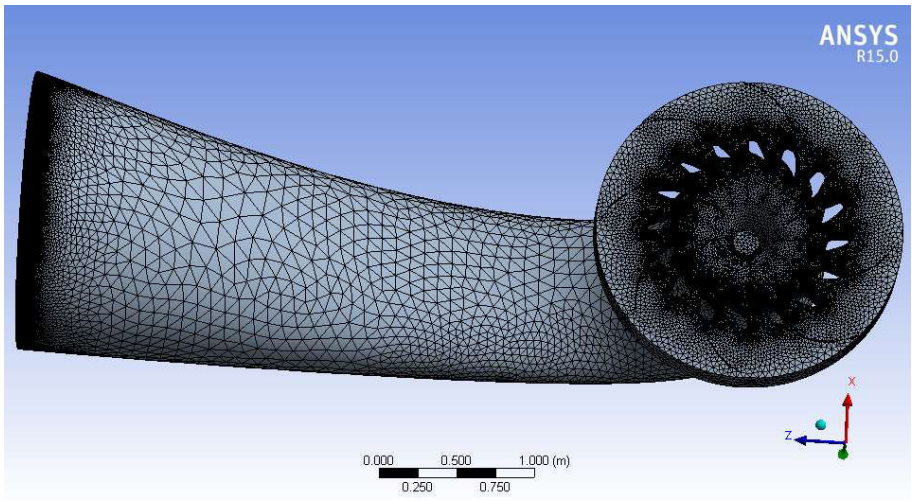

Fig 4.10 Flow domain after mesh refinement

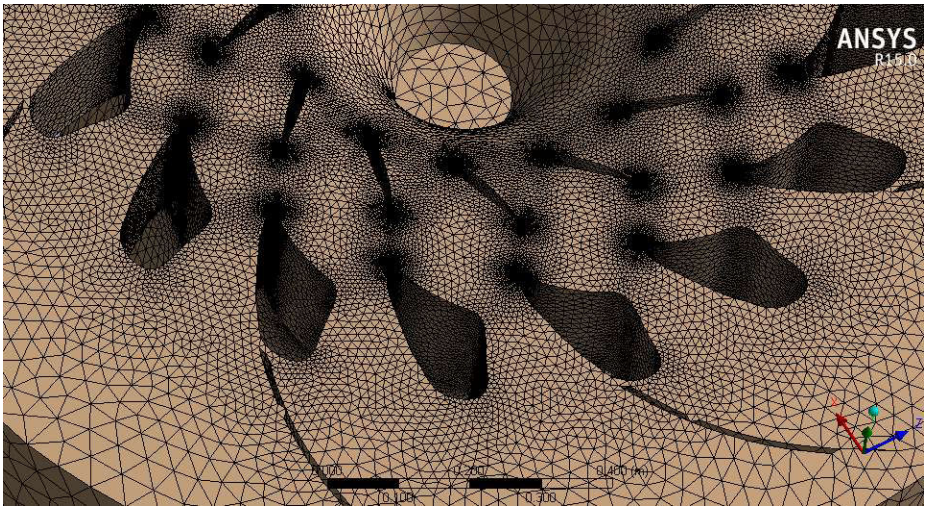

Fig 4.11 Closer view of dense mesh near runner guide vanes and stay vanes

4.3.2 Boundary Selection

To define the direction of flow it is necessary to create a name of each and every surface which will come in contact with water. As ANSYS workbench is name sensitive, therefore proper attention must be taken before assigning the name of flow boundary. The following steps are needed to be followed when assigning the flow boundaries:

- After selecting the appropriate surface and by pressing right click on it lead us to 'create named selection'.
- As the dialogue box appears, typing the appropriate name on the blank space can allow the name selection process. The name selection of turbine runner is shown in Fig 4.12.

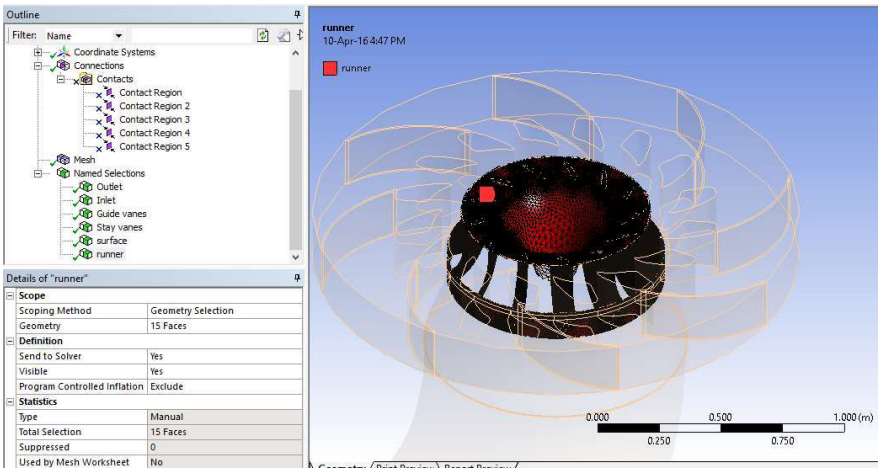

Fig 4.12 Named selection of runner

4.4 MESH STATISTICS

After discretizing the flow domain with unstructured fine tetrahedral mesh the detailed mesh statistics are given for each and every flow domain separately.

(i) Involute casing

Unstructured tetrahedral fine mesh has been created in spiral casing flow domain. The casing consists of 8437 nodes and 39858 elements as shown in the Fig 4.13.

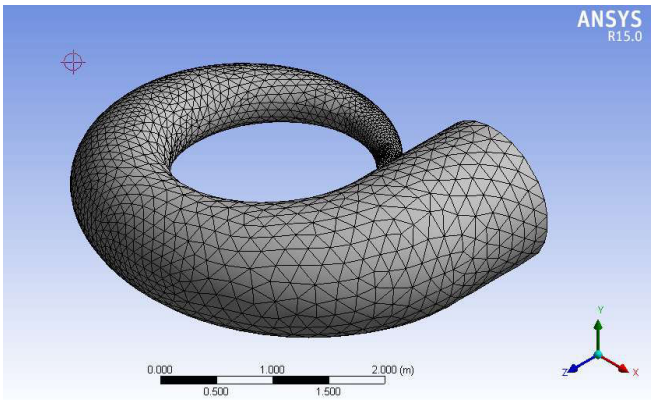

Fig 4.13 Discretized flow domain of casing

(ii) Runner

Unstructured tetrahedral fine mesh has been created in runner flow domain. The casing consists of 44355 nodes and 215897 elements as shown in the Fig 4.14.

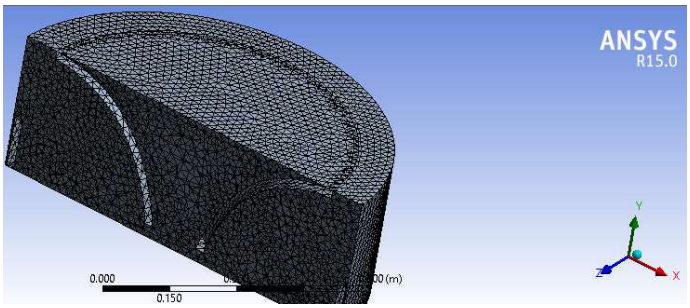

Fig 4.14 Sectional view of discretized flow domain of runner

(iii) Guide vanes and stay vanes

Unstructured tetrahedral fine mesh has been created in guide vanes and stay vanes flow domain. This flow domain region consists of 537839 nodes and 2725974 elements, shown in the Fig 4.15.

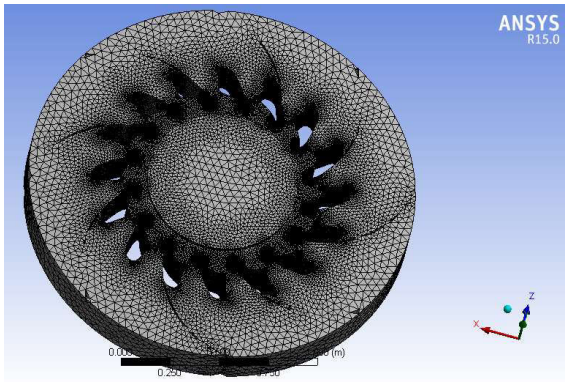

Fig 4.15 Discretized flow domain near guide vanes and stay vanes

(iv) Draft tube

In draft tube section an unstructured tetrahedral fine mesh has been created. In draft tube flow domain there are 46416 numbers of nodes and 211362 numbers of elements has been created, shown in the Fig 4.16.

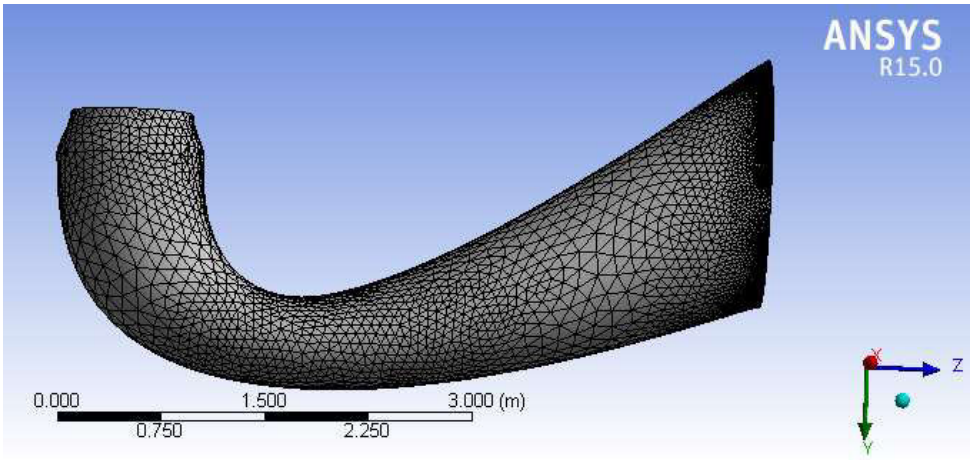

4.16 Discretized flow domain inside draft tube

The overall flow domain consists of 789574 numbers of nodes and 3739040 numbers of elements. After completing the mesh generation with meshing tool, the generated mesh is imported to the 'FLUENT solver'. Before performing simulation in 'FLUENT' the following steps are needed to be followed:

(i) Right click and update the mesh in FLUENT launcher panel in project window of workbench.

(ii) Now in project schematic window, the forth tab is for Setup option. In this setup option the FLUENT launcher can be launched by either double clicking on it or by selecting edit option after pressing right click on it.

(iii) As the FLUENT launcher will appear, it will automatically identify the dimension in 3-D, and for better accuracy select double precision in 'options' radio button. It the system is connected with parallel computing network, then by selecting parallel radio button in processing options will allow several workstations simultaneously to simulate the flow problem, which will reduce the computation time. There is nothing to do with display options.

After launching the FLUENT solver, the computation engine will automatically identify and compute number of nodes and elements in flow domain as shown in the Fig 4.17.

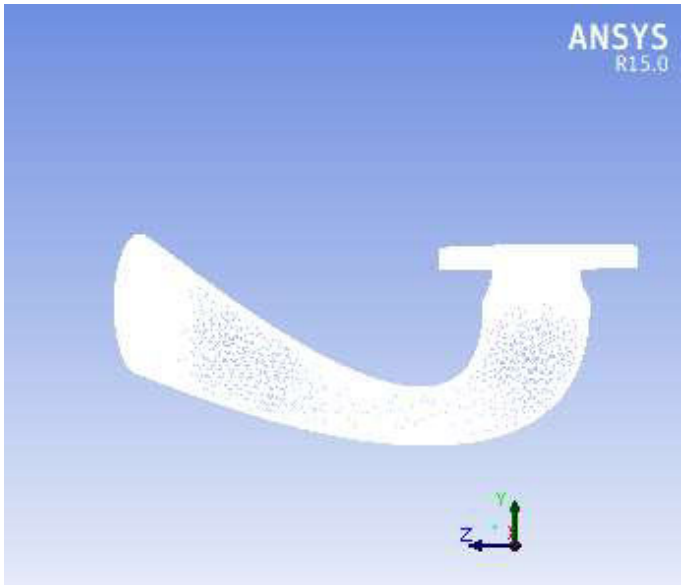

Fig 4.17 Identified flow domain in FLUENT solver

4.5 SIMULATION IN FLUENT

To conduct the computation in FLUENT solver it is very necessary to define the parameters and adopted proper turbulence mode. In this chapter the step by step procedure has been discussed. There are some standard assumption, which are needed to be taken before performing the computation. In this computation process, flow through all sections inside the flow domain are considered to be in steady state. The flowing fluid is considered to be incompressible and in single phase. The all solid surfaces are considered to be smooth and the flow near wall is governed by no-slip condition, which means, there exist a viscous sub-layer near wall.

Steps associated with numerical simulation of Francis turbine are described below. Here the naming of steps are directly taken from FLUENT solution setup tree.

Step 1: General

In this section the refinement of meshing are rechecked. The mesh scale can be optimized again and acceleration due gravity can be defined according to the geometrical orientation of the model. Here in this simulation work the acceleration due to gravity has been taken along +ve z axis and the value is considered 9.81m/s^2.

Step 2: Models

In model section, the user is asked by preprocessor to assign proper turbulence code. In this dissertation work the viscous option of RNG κ-ε has been selected for turbulence flow. Where in RNG option the swirl dominated flow with standard wall function has been selected.

Step 3: Materials

In material selection step the flow domain has been considered with river water at 12°C. The properties of water at 12°C are as follows.

Density 999.5kg/m^3.

Dynamic viscosity 1.234kg/m-s.

Therefore instead of selecting data from FLUENT database, material properties are added in properties option and name has been changed to ‘river-water’. And selecting ‘river-water’ in materials.

Step 4: Boundary Conditions

In boundary condition, the initial conditions and different parameters are assigned with appropriate data, which are collected from plant site given in the Table 4.1.

Table 4.1: Boundary conditions

Components	Data
Inlet velocity	7.51m/s
Runner speed	62.83rad/s
Runner axis of rotation	Along y axis
Gauge pressure at exit	0Pa

After assigning the initial and final values to the boundary condition, the reference values should be chosen as computation from inlet and the reference zone will be solid.

Here in this computation technique the solution scheme has been chosen as PISO, where skewness correction and neighbor correction factors has been assumed as unity.

In calculation activities the auto save iterations are taken as after every 10 successive iteration. And in run calculation the number of iteration are taken hundred where reporting iteration is been assigned in every 10 successive iterations. Then finally hitting the run calculation option will trigger the iteration. In scaled residuals graphical presentation gives us a scope to visualize the convergence of solution. Here in this complex flow domain the computation time consumed by the FLUENT for each guide vane position is about 2hour 45minnutes in an Intel core i3 4005U processor with 1.70GHz maximum clock speed with 4GB DDR3 RAM and 2GB NVIDIA GeForce 820M GPU configuration. After finishing the calculations the user needs to open FLUENT CFD-Post to visualize the flow nature in various domain as shown in the Fig 4.18.

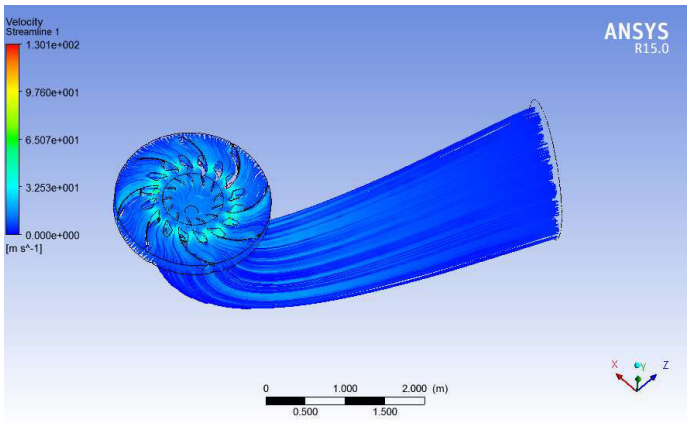

Fig 4.18 Velocity stream function through turbine setup

CHAPTER 5
RESULTS AND DISCUSSION

5.1 GENERAL

A numerical investigation of complex flow through Francis turbine has been investigated with using swirl dominated RNG- κ-ε turbulence model for different guide vane opening position. The flow nature in various sections of turbine, their velocity and pressure variations are also discussed in this chapter. The efficiency and operating characteristics are as discussed in the subsequent paragraph of this chapter. Farther a comparison study has been made at the end of this chapter.

5.2 NUMERICALLY INVESTIGATED FLOW FIELD

During the CFD based performance investigation of the Francis turbine, the CAD model was generated on full-scale design. Therefore the flow nature shown through the model will be quite exact in nature with actual prototype. Here the simulation was performed with constant speed of runner at 600 rpm and flow variations was 3.10m³/s to 5.28m³/s, i.e. from fully open guide vane position to fully closed position. Here the head variation has been neglected. The numerical investigation on different parts of the turbine has been carried out by assigning inlet flow velocity, exit pressure and constant mass flow rate at the exit of draft tube.

The overall efficiency has been calculated from the standard formula shown in equation 2.3, where P is power output from turbine and H is available net head. The power can be calculated by using formula as below:

$$P=\omega x T \tag{5.1}$$

Where T is the torque generated by the turbine to run the generator shaft in N-m and ω is angular seed in rad/s.

5.3 VEOCITY AND PRESSURE CONTOUR AT DESIGNED CONDITION

At designed condition the velocity and pressure variation in different sections of turbine setup is necessarily be under critical working condition. The pressure inside the hydraulic circuit must not be below the vapour pressure of water at that temperature and atmospheric pressure. FLUENT CFD-Post tool helps us to map the velocity stream function contour and pressure contour inside the flow domain with color intensity variation. Therefore it easily short out the cavitation prone

zone inside the flow domain and leads us to identify the critically running fluid zone in flow circuit. From Fig 5.1 to 5.3 the variation of pressure contour and from Fig 5.4 to 5.6, velocity contour has been shown for various sections. A combined velocity and pressure contour is shown in Fig 5.7.

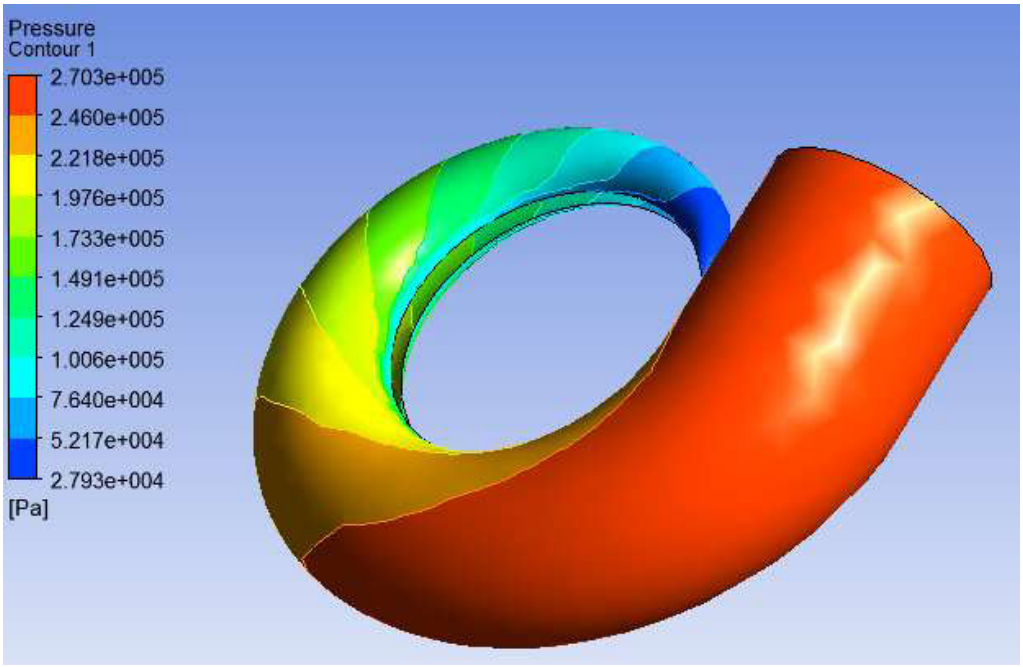

Fig 5.1 Pressure contour in involute casing

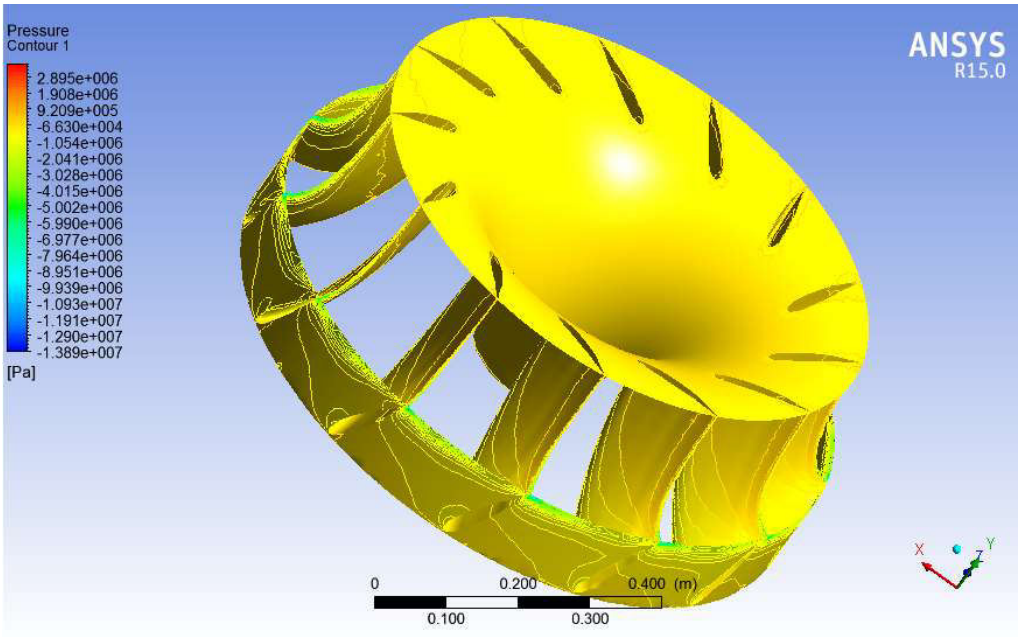

Fig 5.2 Pressure contour in runner

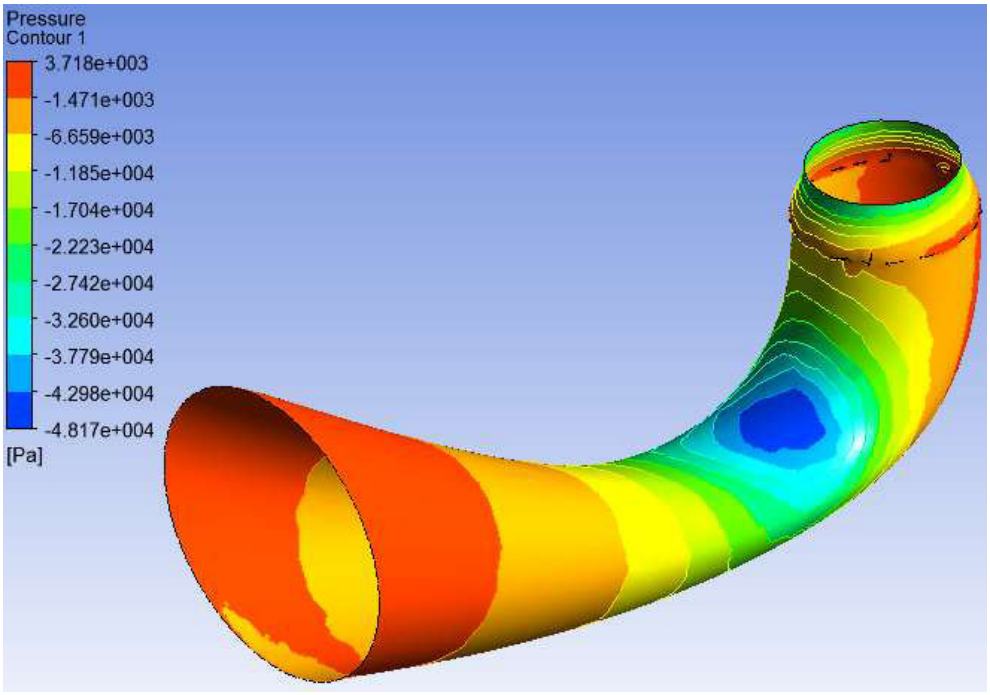

Fig 5.3 Pressure contour in draft tube

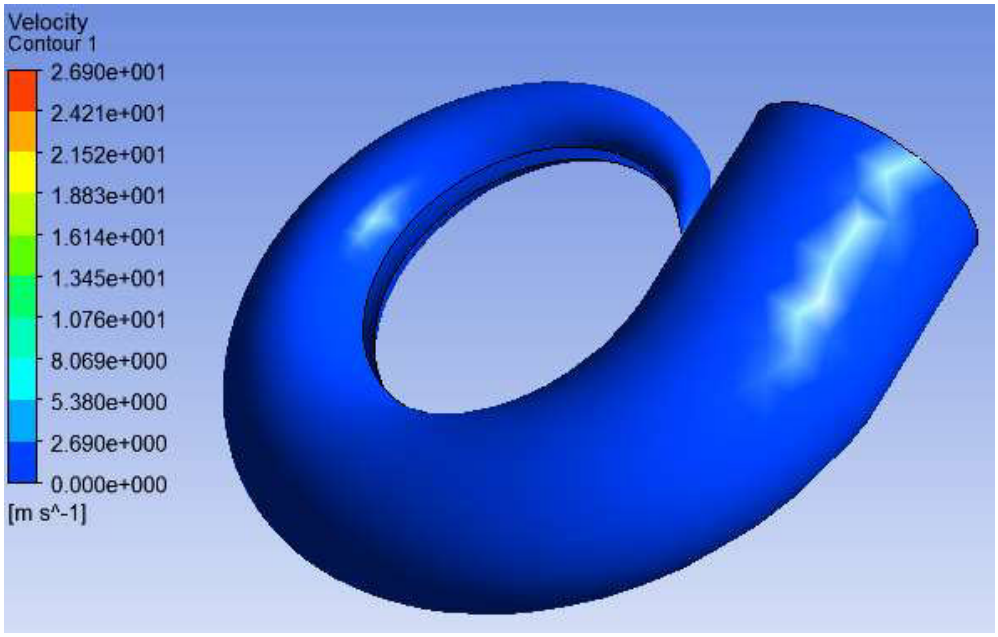

Fig 5.4 Velocity contour in involute casing

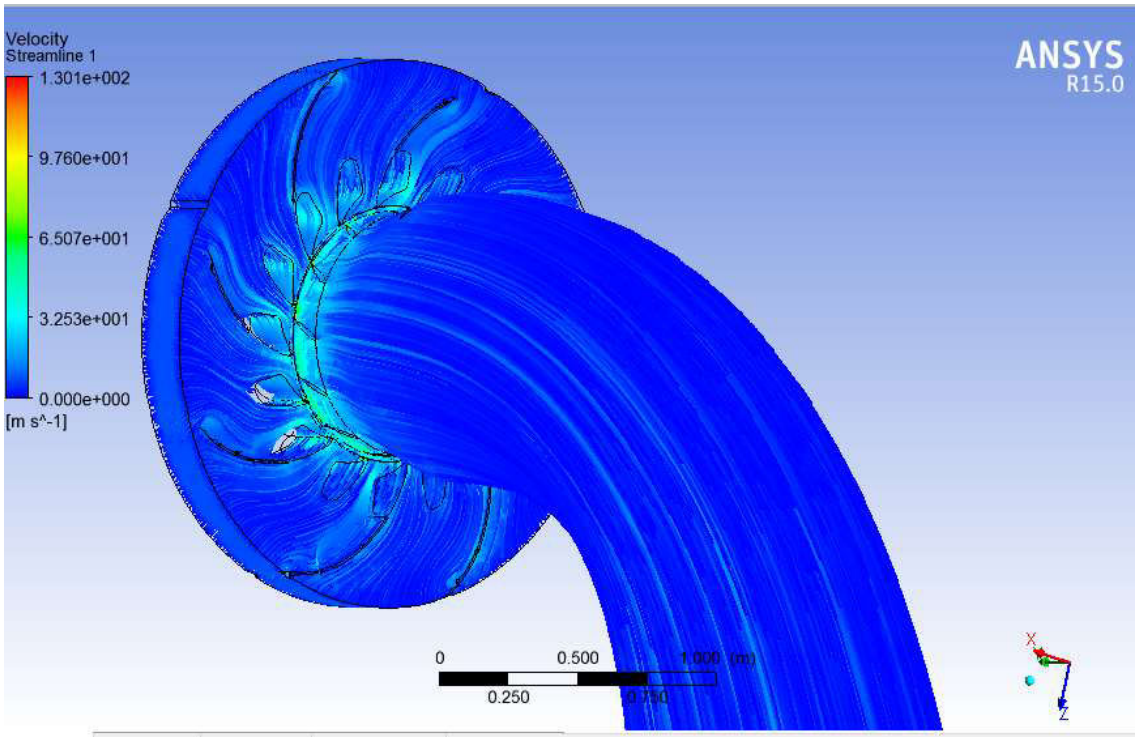

Fig 5.5 Velocity variation near stay vanes guide vane and runner

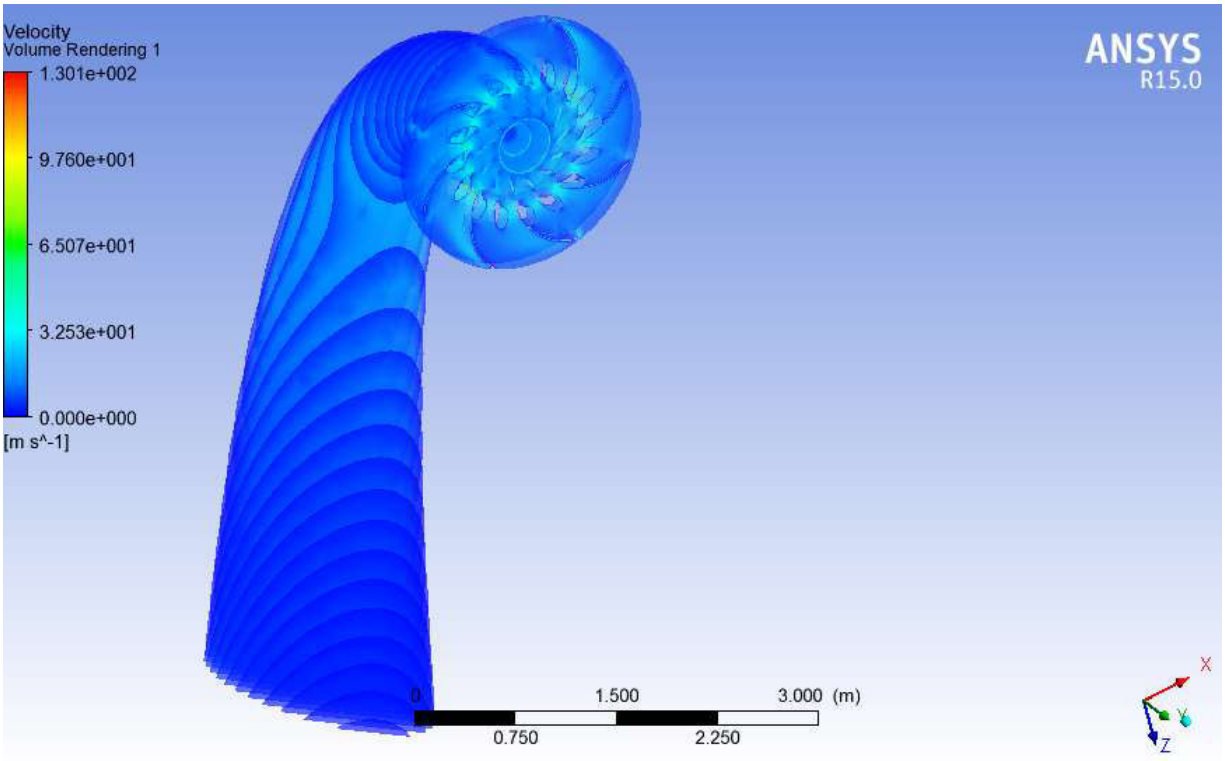

Fig 5.6 Complete velocity contour in flow domain

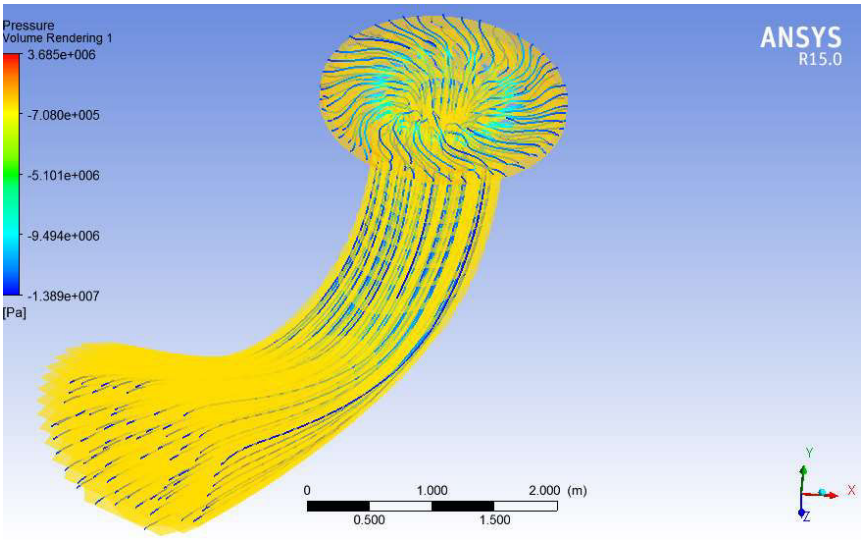

Fig 5.7 stream line and pressure variation in flow domain

5.4 RESULTS

The output torque generated by turbine under different guide vane opening position are discussed below. For the calculation purpose the input and output parameters are given in tabulated form. A comparison study has been done with graphical representation.

5.4.1 Input Parameters

Under constant speed of runner at 600 rpm the flow variation through different guide vane opening position, the discharge rate and corresponding available potential has been given in the Table 5.1 where net head is 46.65m, which remains constant.

Table 5.1: Input parameters

S.NO.	Guide Vane Angle	Discharge Rate (m^3/s)	Pressure at Draft tube Exit(Pa)	Potential (kW)	Runner Speed(rad/s)
1	24.50°	3.10	104718	1417.96	62.83
2	32.60°	3.9	104718	1783.89	62.83
3	36.70°	4.30	104718	1966.85	62.83
4	40.80°	4.80	104718	2195.55	62.83
5	44.88°	5.28	104718	2415.11	62.83

The exit of the draft tube is under atmospheric pressure.

5.4.2 Output Parameters

Solving the Navier-Stokes equation and continuity equation on the basis of initial boundary conditions at different guide vane opening positions the output torque has been computed by the FLUENT. During the solving process the head has been considered constant. Momentum transfer by the water flow to runner creates three dimensional torque in turbine shaft. The Output in a form of generated torque is given below in Table 5.2.

Table 5.2: Output parameters from solver

S.NO.	Guide Vane Angle	Torque(kN-m)	Power Output(kW)	Efficiency
1	24.50°	19.07	1198.17	84.50%
2	32.60°	25.21	1619.95	90.81%
3	36.70°	28.77	1846.87	93.90%
4	40.80°	32.43	2066.01	94.10%
5	44.88°	34.27	2177.22	90.15%

5.4.3 Efficiency versus Flow Rate

The observed results give us a clear idea about the relationship between discharge rate and efficiency of Francis turbine. It can easily be seen from Table 5.2 that, although the rated power output from turbine is higher at 44.88° guide vane opening position than 40.80° guide vane opening position, but the efficiency at this point is quite low than best efficiency point (BEP), which can be observed at 40.80° guide vane opening position. The graph of discharge rate versus efficiency is shown in the Fig 5.8.

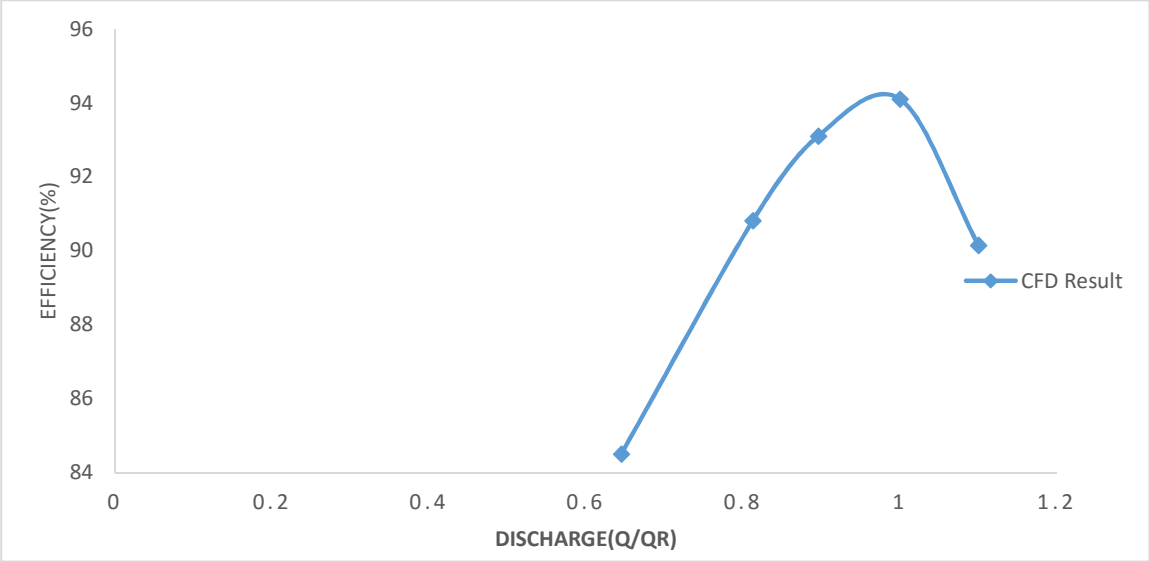

Fig 5.8 CFD result for efficiency against discharge

5.4.4 Comparison Study between CFD and Available Results

It is very important task to validate the CFD result with experimented results. Therefore a comparison study has been made to verify the results. Both CFD analyzed data and available data are given below in Table 5.3.

Table 5.3: Comparison between CFD efficiency and available efficiency at different guide vane opening position

S.NO.	Guide Vane Angle	Discharge Rate	Available Efficiency	CFD Efficiency
1	24.50	3.10	85.50%	84.50%
2	32.60	3.90	90.50%	90.81%
3	36.70	4.30	92.40%	93.90%
4	40.80	4.80	93.20%	94.10%
5	44.88	5.28	92.50%	90.15%

A comparison of efficiency has been made on the basis of discharge data against available efficiency and CFD efficiency. Both efficiencies are given in Table 5.3 above and a graphical representation is shown in Fig 5.9. From the Fig 5.9 it can be seen that CFD results are in good agreement with available plant site data, which validates the CFD based performance analysis, but

also suggests some improvements in runner design to improve efficiency. At above rated discharge condition significant deviation on efficiency can be observed in CFD result. This deviation and variation in results may be caused due to either measurement error or due to some standard assumptions made during design stage.

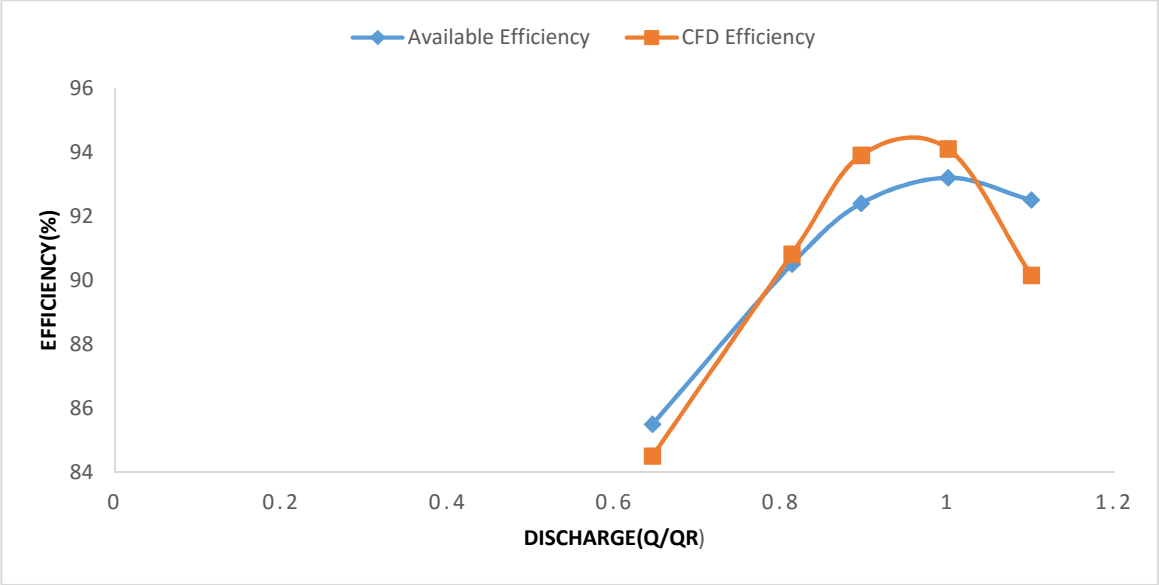

Fig 5.9 Comparison between CFD efficiency and available efficiency

The comparison study made in the Table 5.3 suggests that, at 4.80m³/s rated discharge the efficiency achieved by CFD experiment differs by 1% in maximum available efficiency. It can be seen from the graphical comparison made in Fig 5.9 that, at three different discharge conditions, i.e. at 3.90m³/s 4.30m³/s and 4.80m³/s, CFD results give better efficiency than available efficiency from plant site data. The drastic variation in efficiency can be observed beyond operating point. Which accepts the general property of Francis's poor part load efficiency. Although a variation between available data and CFD data can be observed, but the variations are very minute and nature of CFD curve has a good agreement with available efficiency curve of that turbine.

CHAPTER 6
CONCLUSIONS AND RECOMMENDATIONS

6.1 CONCLUSIONS

The CFD based performance analysis carried out under the present study verifies that the Francis turbine is an efficient hydro turbine in its full load capacity. It runs poorly at below rated discharge and beyond operating condition. In this dissertation an attempt has been made to verify the performance of a Francis turbine with the help of computational fluid dynamics. It is found that RNG κ-ε turbulence model gave better results to predict the behavior of flow through turbine runner and other hydraulic components. The following conclusions are been made from the present dissertation work:

i. A Francis turbine working under 46.65m head and running at 600rpm between 3.10m^3/s to 4.80m^3/s discharge has been selected for the present investigation work.

ii. Detailed dimensioning of casing, guide vanes, guide vanes, runner and draft tube have been modeled in Solidworks 3-D modeler. IS 7418-1991[26] and IS 5496-1993 [30] has been followed for casing and draft tube designing purpose. For stay vane and guide vane designing a standard manual by Lulea University of Technology [29] has also been followed.

iii. 3-D model of Francis turbine setup was designed in Solidworks was imported to ANSYS for CFD simulation in a PARASOLID (.t_x) format which provides great accuracy and flexibility in design model.

iv. Although a huge computation time and advanced machine is needed to perform the flow simulation, but the computation accuracy is significantly high in RNG κ-ε turbulence model.

v. The analyzed results for maximum efficiency are compared with available data, which differ by about 1% to the available maximum efficiency. This may be caused due to some measurement error or due to some standard assumption made during predesign planning in this study.

6.2 RECOMMENDATIONS

i. A performance analysis of Francis turbine can be made by using more advanced computation code in a more powerful machine.

ii. The deviation of results caused due to some standard assumption made during design process, can be eliminated by collecting more data from the plant site.

iii. Although a fine unstructured tetrahedral mesh has been created during discretization process, but denser and finer hexahedral mesh can be used to eliminate the deviation in results and provide a more accurate results.

REFERENCES

[1] <http://www.iea.org/publications/freepublications/publication/hydropower_essentials.pdf> accessed on 02/04/16.

[2] <https://www.worldenergy.org/data/resources/resource/hydropower/> accessed on 02/04/16

[3] <http://cea.nic.in/reports/monthly/executivesummary/2016/exe_summary-02.pdf>accessed onv02/04/16.

[4] PwC report on Hydropower in India, titled “Hydropower in India Key enablers for a better tomorrow”.

[5] <http://mnre.gov.in/schemes/grid-connected/small-hydro/> accessed on 27/09/15

[6] MNRE report on “STATE WISE NUMBERS AND AGGREGATE CAPACITY OF SHP PROJECTS (UPTO 25 MW)” as on 31.03.2014.

[7] Dritina P, Sallabarge M., “Hydraulic turbines — basic principles and state-of-the art computational fluid dynamics applications” Journal of Mechanical Engineering Science, Zurich, Volume 213 (Published 1998)

[8] Hasan Akin., Zeynep Aytac., Fatma Ayancik., Ece Ozkaya., Emre Arioz., Kutay Celebioglu., Selin Aradag., “A CFD Aided Hydraulic Turbine Design Methodology Applied to Francis Turbines”, Journal of Mechanical Engineering TOBB University of Economics and Technology;(Retrieved on: 21 August 2015)

[9] Shukla M K, Jain R, Prof. Prasad V, Shukla S N,. "CFD Analysis of 3-D Flow for Francis Turbine", MIT International Journal of Mechanical Engineering; Volume 1, pp.99-100,Aug 2011

[10] Patel K, Desai J, Chauhan V, Charnia S., "Development of Francis Turbine using Computational Fluid Dynamics". Asian International Conference on Fluid Machinery and Fluid Power Technology Exibition; Chennai,November 21-23, 2011

[11] Lain S., Garcia M., Quintero B., Orego S., "CFD Numerical simulation of Francis turbine". Universidad De Antioquia; Volume 51,pp.24-33, February 2010

[12] Ying HU., Heming C., Ji HU., Xirong LI., "Numerical Simulation of Unsteady Turbulent Flow through a Francis Turbine". Wuhan University Journal of Natural Sciences; Volume.16,pp.179-184,2011

[13] Khare R., Prasad V., "Numerical Study of Peformance Characteristics of Draft tube of Mixed Flow Hydraulic Turbine", Hydro Nepal; Issue 10,January 2012

[14] Ayancik F., "A CFD Aided Hydraulic Turbine Design Methodology Applied to Francis Turbine", Journal of Mechanical Engineering TOBB University of Economics and Technology;(Received August 2015)

[15] Kaewnai S., Wongwises S., "Improvement of the Runner Design of Francis Turbine using Computational Fluid Dynamics",American Journal of Engineering and Applied Science;ISSN 1941-7020,pp.540-547,2011

[16] Oh HW., Yoon ES., "Application of Computational fluid dynamics to performance analysis of a Francis hydraulic turbine", Journal of Institution of Mechanical Engineers; Volume 221,pp.583-590,2007

[17] Carija Z., Mrsa Z., Fucak S., "Validation of Francis Water Turbine CFD Simulations" Journal of Association for Engineering mechanics; Issue 50,pp. 5-14,2008

[18] Firoozabadi B., Dadfar R., Pirali AP., Ahmadi G., "Effect of Different Geometries in Simulation of 3D Viscous Flow in Francis Turbine Runners". Sharif University of Technology;Volume 16,pp.363-369,August 2009

[19] Krappel T., Ruprecht A., Riedelbauch S., Zuerker RJ., Jung A., "INvestigation of Francis turbine Part Load Instability using Flow Simulations with a Hybrid RANS-LES Turbulence Model".Journal on Hydraulic Machinery and Systems(IAHR-2014) IOP Publishing; Volume 22,pp.1-10,2014

[20] Jošt D., Škerlavaj A., Turboinštitut AL., "Improvement of Efficiency Prediction for a Kaplan Turbine with Advanced Turbulence Models". Journal of Mechanical Engineering; pp 124-134, 2014

[21] Agostani Neto AD., Zuerker RJ., Jung A., Maiwald M., "Evaluation of a Francis turbine daft tube flow at part load using hybrid RANS-LES turbulence modelling". Journal on Hydraulic Machinery and Systems (IAHR-2012) IOP Publishing;Volume 15,Issue 26,pp.1-10,2012

[22] Foroutan H., Yavuzkurt S., "Unsteady Numerical Simulation of Flow in Draft Tube of a Hydroturbine Operating Under Various Conditions Using a Partially Averaged Navier–Stokes Model", ASME Journal of Fluids Engineering; Volume 137, pp.061101-1, 2015

[23] < http://elearning.vtu.ac.in/P6/enotes/CV44/Char_Cur-MNSP.pdf> accessed on 02/04/16

[24] Avellan F., “Introduction to Cavitation in Hydraulic Machinery” 6th International conference on Hydraulic Machinery and Hydraulics; Politehnica University of Timisoara, Timisoara, Romania, October 2004

[25] Gohil Pankaj P., Saini R.P., " CFD: Numerical Analysis and Performance Prediction in Francis Turbine", 1st International Conference on Non-Conventional Energy (ICONCE 2014); pp.94-97, January 2014.

[26] IS 7418:1991(Reaffirmed 2003) "Criteria for Design of Spiral Casing (Concrete and steel)".

[27] < https://en.wikipedia.org/wiki/Francis_turbine> accessed on 02/06/15

[28] MANUAL "HYDROPOWE IN NORWAY Mechanical Equipment"; Norwegian University of Science and Technology.

[29] <http://www.ltu.se/research/subjects/Stromningslara/Konferenser/Francis-99/Test-Case-1.111520?l=en > accessed on 01/06/15

[30] IS 5496:1993 (Reaffirmed 2003) "Guide for Preliminary Dimensioning and Layout of Elbow Type Draft Tubes for Surface Hydraulic Power Stations".